



## A study on the hepatic response to heat stress in *Gymnocypris eckloni* through an approach combining metabolomic and transcriptomic profiling

Chaowei Zhou<sup>a,b,1</sup>, Yuting Duan<sup>a,b,1</sup>, Junting Li<sup>a,b</sup>, Suxing Fu<sup>a,b</sup>, Shuhao Bai<sup>a,b</sup>, Yutong Zhuang<sup>a,b</sup>, Shidong Liu<sup>a,b</sup>, Hejiao Li<sup>a,b</sup>, Yinhua Zhou<sup>a,b</sup>, Qiming Wang<sup>c</sup>, Jian Shen<sup>d</sup>, Rongzhu Zhou<sup>e,\*</sup>, Luo Lei<sup>a,b,\*</sup>, Haiping Liu<sup>a,\*</sup>

<sup>a</sup> Integrative Science Center of Germplasm Creation in Western China (CHONGQING) Science City & Southwest University, Chongqing, China

<sup>b</sup> College of Fisheries, Southwest University, Chongqing 400715, China

<sup>c</sup> Department of Agriculture and Rural Affairs of the Xizang Autonomous Region, Xizang 850000, China

<sup>d</sup> Huadian Xizang Energy Co., Ltd., Xizang 851414, China

<sup>e</sup> National Animal Husbandry Services, Beijing 100125, China

### ARTICLE INFO

#### Keywords:

*Gymnocypris eckloni*  
Heat stress  
Transcriptome analysis  
Metabolome analysis

### ABSTRACT

*Gymnocypris eckloni*, an economically important cold-water fish widely cultivated in southwest China, is at increased risk of prolonged exposure to heat stress owing to persistent high temperatures in summer, extreme climate changes, and expansion of factory farming. In this study, *G. eckloni* was subjected to both chronic and acute heat stress, with subsequent analysis focusing on changes in the pathological and physiological characteristics and transcriptomic and metabolic responses of the liver to high temperature. The results revealed heat stress-induced damage to liver tissues, lipid accumulation and mitochondrial abnormalities in hepatocytes, and an increased number of apoptotic cells, with the damage being more severe under acute heat stress conditions. Assessment of biochemical indices showed that the antioxidant enzyme catalase (CAT) was activated in response to oxidative stress and energy demands increased following heat stress. Transcriptomic analysis showed significant enrichment in the protein processing in the endoplasmic reticulum pathway, along with upregulation of key genes associated with protein degradation (*hsp40*, *hsp70*, *hsp90*, *ero1l*, and *pdia4*) and activation of the unfolded protein response (UPR), which effectively reduces or clears the accumulation of misfolded proteins to combat stress. Most identified differential metabolites were associated with amino acid and lipid metabolism under heat stress. Notably, integrated transcriptomic and metabolomic analysis suggested that tryptophan metabolism played an important role in the adaptation of *G. eckloni* to chronic heat stress. These findings improve the understanding of the mechanisms through which *G. eckloni* adapts to high temperatures, providing a valuable foundation and novel avenues for developing strategies to alleviate the effects of heat stress and improve the outcomes of aquaculture.

### 1. Introduction

Temperature is an important environmental factor in aquaculture, exerting profound effects on the growth, development, metabolism, immunity, and reproduction of various fish species (Lu et al., 2016; Mahanty et al., 2019; Mahmoud et al., 2020). Although fish possess mechanisms to regulate their internal environment in response to temperature fluctuations, significant deviations from optimal ranges or abrupt fluctuations can disrupt these mechanisms, leading to severe

tissue damage or death (Huang et al., 2018; Wang et al., 2019). Owing to persistent high temperatures in summer, increasing occurrences of extreme climate events, and the expansion of factory farming practices, fish within aquaculture systems are at increased risk of prolonged exposure to heat stress, which presents a formidable challenge to aquaculture technology and industrial development, particularly for cold-water fish species (Alfonso et al., 2021). Consequently, understanding the mechanisms through which fish adapt to heat stress is a major focus of current research in the field of aquaculture.

\* Correspondence to: College of Fisheries, Southwest University, Chongqing, China.

E-mail addresses: [1109904665@qq.com](mailto:1109904665@qq.com) (R. Zhou), [leiluo12311@163.com](mailto:leiluo12311@163.com) (L. Lei), [luihappy@163.com](mailto:luihappy@163.com) (H. Liu).

<sup>1</sup> Joint first authors.

A fundamental approach to investigating the impact of heat stress on fish involves the assessment of morphological features and biochemical indicators (Ma et al., 2020). Notably, studies on *Oreochromis niloticus* (Mahmoud et al., 2020) and *Apostichopus japonicus* (Wang et al., 2021) have shown that heat stress causes damage to ovarian and intestinal tissues. Additionally, exposure to high temperatures leads to changes in blood biochemistry, induces oxidative stress, activates antioxidant defenses, disrupts energy metabolism, and alters the levels of glucose and fatty acids (Mahmoud et al., 2023; Bao et al., 2018; Kühnhold et al., 2017; Li et al., 2022, 2019; Liu et al., 2023). With the use of advanced omic technologies, dynamic changes caused by heat stress can be comprehensively analyzed at the transcriptomic, metabolomic, or proteomic levels. In studies on *Haliotis discus hannai* (Wu et al., 2023), *Sebastes marmoratus* (Han et al., 2023), and *Epinephelus fuscoguttatus* (Duan et al., 2024), transcriptomic analysis has been used to identify major regulatory genes and pathways that mitigate heat stress in fish. Furthermore, metabolomic analysis of *Brachymystax lenok* has shown that accumulation of L-carnitine and acylcarnitine ester glycerophospholipids may play a role in alleviating oxidative stress (Chen et al., 2022). Similarly, metabolomic analysis of *Micropterus salmoides* has demonstrated that administration of steroidal saponins can improve hepatic lipid metabolism under heat stress (Cheng et al., 2023). Although metabolomic analysis has been extensively used in studies on mollusks, such as clams and scallops, under heat stress, its application in studies on fish remains relatively limited (Jing et al., 2023; Li et al., 2022). In a study on *Triplophysa siluroides*, integrated metabolomic and transcriptomic analysis showed that enhanced purine metabolism served as a protective mechanism against cellular damage caused by heat stress (Chen et al., 2023b). Therefore, the combined use of transcriptomic and metabolomic analyses may offer insights into regulatory mechanisms linking genes and metabolites, thereby allowing a better approach to elucidating the effects of heat stress on cold-water fish species.

The liver plays an integral role in excretion, metabolism, and detoxification in fish (Qin et al., 2023). Consequently, dynamic changes in the liver may reflect the physiological status of fish. The liver is highly susceptible to environmental stress, making it a prominent target in studies on environmental monitoring and stress response (Hazel, 1979). As a central site of nutrient metabolism, the liver plays an essential role in metabolic reprogramming in response to stress, maintaining energy homeostasis by orchestrating the interactions among carbohydrate, protein, and lipid metabolic pathways (Ma et al., 2020; Zhang et al., 2022). Studies have shown that acute or chronic heat stress induces significant alterations in the tissue structure and metabolic responses of the liver (Liu et al., 2016). Following heat stress, the body produces excessive reactive oxygen species (ROS), triggering oxidative stress and lipid peroxidation (Wang et al., 2019), a phenomenon closely related to the liver's role as the primary site of lipid metabolism (Sissener et al., 2017). Upon exposure to high temperatures, the body accelerates the conversion of liver glycogen to glucose, increasing blood glucose levels to fulfill energy storage and supply demands. In recent years, the molecular mechanisms and metabolic reactions involved in heat acclimatization have been investigated in the livers of fish species such as *Seriola lalandi* (Liu et al., 2021), *Glyptosternum maculatum* (He et al., 2023), *Lateolabrax maculatus* (Cai et al., 2020), and *Salmo salar* (Sissener et al., 2017). Consequently, the liver is recognized as a key metabolic organ closely associated with the heat stress response in fish (Li et al., 2017).

*Gymnocypris eckloni*, a prominent member of the subfamily Schizopsidae, primarily inhabits the upper reaches and tributaries of the Yellow River in China (Tang et al., 2015). This species holds ecological importance, contributing to the freshwater ecosystem of the plateau and serving as a crucial aquatic wildlife germplasm resource in Qinghai province, China (He et al., 2024). Moreover, *G. eckloni* is esteemed for its delicious taste, high nutritional value, and consumer popularity, serving as an economically important cold-water fish (Li and Deng, 2014). Since the advent of artificial propagation in Qinghai and Sichuan provinces of

China in 2008, *G. eckloni* has emerged as a commercially important species and is extensively cultured in southwest China (Tang et al., 2015; Yang et al., 2017). However, the constraints imposed by changes in water temperature limit its artificial culture. The optimal temperature for the growth and reproduction of *G. eckloni* is 16–18°C, beyond which its growth rate diminishes (Jian et al., 2020). High temperatures pose a substantial threat to *G. eckloni*, potentially leading to abnormal behavior and cardiac structural damage (Li et al., 2024). Owing to the progressive increase in temperatures in summer and extreme climate changes, heat stress poses a major threat to the culture of *G. eckloni*, a challenge exacerbated by the expansion of factory farming practices. Although studies have reported on various aspects of *G. eckloni*, including growth characteristics (Wang et al., 2022), acclimatization to hypoxia (Zhao et al., 2018), phylogeny (Bao et al., 2023), metal stress (Ran et al., 2021) and gene expression profiles (Zhang et al. n.d.), studies investigating its response to high stress remain limited. In this study, we subjected *G. eckloni* to chronic and acute heat stress and subsequently assessed liver tissue damage by analyzing the histological, morphological, and apoptotic features of the liver and monitoring changes in various serum and liver biochemical indices. Furthermore, we investigated the regulatory mechanisms underlying the heat stress response at the transcriptomic and metabolomic levels. The findings may enhance the understanding of the adaptive mechanisms of *G. eckloni* in response to heat stress, offering a valuable reference and novel avenues for developing strategies aimed at minimizing the adverse effects of heat stress and improving the outcomes of aquaculture.

## 2. Materials and methods

### 2.1. Fish grouping and heat stress treatment

*G. eckloni* (weight, 260 ± 20 g) was obtained from Chuanze Fisheries Corporation (Sichuan, China) and transported to the laboratory at College of Fisheries, Southwest University. The fish were randomly divided into three groups, with three replicate tanks in each group and 15 fish in each tank. They were cultured in rectangular glass tanks equipped with electric heaters and thermometers. The overall water temperature was maintained at 16°C using a Gemei inverter chiller thermostat (BBX-2PH, China). Throughout the experiment, the fish were fed three times daily and were maintained at a pH of 6.5–6.8, with dissolved oxygen levels of > 5 mg/L. Water quality parameters were measured using the AZ86031 water quality tester (AZ Instrument Corp., Guangdong, China). After 1 week of acclimatization, the three groups were designated as follows: control group (CG), in which the water temperature was maintained at 16.0 ± 0.5°C; acute heat stress (AH) group, in which the water temperature was increased 2°C per hour until it reached 28.0 ± 0.5°C and was maintained for 12 h (Dagoudo et al., 2023; Guo et al., 2020; Liu et al., 2023); and chronic heat stress (CH) group, in which the water temperature was increased 2°C per day until it reached 28.0 ± 0.5°C and was maintained for 2 weeks (Giroux et al., 2019; Kim et al., 2019; Naz et al., 2023). This study was approved by Southwest University's animal research protocols and conducted in accordance with the guidelines established by the Institutional Animal Care and Use Committee of Southwest University.

### 2.2. Sample collection

A total of 9 fish randomly selected from each treatment group were anesthetized using 40 mg/L MS-222 (Sigma, USA). After blood was collected using 1 mL disposable syringes, the liver was harvested and divided into four sub-samples. The first sub-sample was fixed in 4 % paraformaldehyde for histopathological analysis and apoptosis assay; the second sub-sample was fixed in 2 % glutaraldehyde for morphological analysis of hepatocytes; and the third and fourth sub-samples were promptly frozen in liquid nitrogen and stored at –80°C for transcriptomic and metabolomic analyses, respectively.

### 2.3. Histopathological analysis

After 24 h of fixation, the liver tissues were successively dehydrated in a graded series of ethanol solutions (70 %, 85 %, 95 %, and 100 %), cleared with xylene, embedded in paraffin, and cut into 5- $\mu$ m-thick sections. These sections were stained with hematoxylin and eosin (Solarbio, Beijing, China) and sealed with neutral gum. The sections were observed and photographed using a microscope (CX41, Olympus, Japan) equipped with a microscope imager (DMD108, Leica, Germany). For each group, the total number of nuclei was counted in five non-overlapping randomly selected visual fields under 40.0x magnification.

### 2.4. Morphological analysis of hepatocytes

Liver tissue samples were fixed in 2.5 % glutaraldehyde for 4 h, followed by post-fixation in 1 % osmium tetroxide ( $\text{OsO}_4$ ) for 1 h at 4°C. After the tissues underwent a series of dehydration steps, they were embedded in the Epon812 epoxy resin and cut into 70- $\mu$ m-thick slices using an RMC PowerTome XL microtome. These slices were stained with uranyl acetate and lead citrate and examined using the Hitachi H-7650 transmission electron microscope (Hitachi, Tokyo, Japan).

### 2.5. Apoptosis assay

Apoptotic cells in the liver were detected using the TUNEL Apoptosis Assay Kit (Solarbio, Beijing, China). Briefly, the liver tissue sections were deparaffinized, rehydrated with ethanol, and treated with proteinase K for 30 minutes at 37°C. Subsequently, the sections were treated with a labeling solution comprising terminal deoxynucleotide transferase, a buffer, and fluorescein dUTP for 2 h at 37°C and stained with DAPI. Finally, the sections were observed under a fluorescence microscope (Eclipse50i, Nikon, Japan), and the viability of liver cells was quantified using the ImageJ software, an image analysis software developed by the National Institutes of Health, USA.

### 2.6. Assessment of biochemical indices

Blood samples were stored at 4°C for 12 h and subsequently centrifuged at 5000 rpm for 15 minutes. The supernatant was collected for the detection of alanine aminotransferase (ALT), aspartate aminotransferase (AST), glucose (D-Glc), and cortisol. Frozen liver tissue samples were used for oxidative stress analysis, focusing on the detection of malondialdehyde (MDA), superoxide dismutase (SOD), and catalase (CAT), and energy metabolism analysis, focusing on the detection of glycogen, ATPase, triglycerides (TGs), and total cholesterol (TC). In addition, fresh liver tissue samples were immediately used for ROS assay. ROS levels were measured using a fluorescent probe and microplate reader (EPOCH-SN, Gene Company Limited, China). All biochemical indices were measured using commercial assay kits obtained from ZCIBIO Technology Co., Ltd., China, according to the manufacturer's instructions.

### 2.7. Transcriptomic analysis

Total RNA was extracted from liver tissues using the FastPure Cell/Tissue Total RNA Isolation Kit V2 (Vazyme, Nanjing, China) following the manufacturer's protocol ( $n = 3/\text{group}$ ). RNA concentration was determined through agarose gel electrophoresis, and the RNA integrity number (RIN) was assessed using the Agilent 2100 Bioanalyzer (Agilent Technologies, CA, USA). Subsequently, a cDNA library was constructed using the NEBNext Ultra™ RNA Library Prep Kit for Illumina (NEB, USA). After purification, the cDNA library was sequenced on the Illumina Novaseq6000 platform by Gene Denovo Biotechnology Co., (Guangzhou, China). Raw reads were filtered using fastp (version 0.18.0) to acquire high-quality clean reads. The sequences obtained from bipartite sequencing were aligned to the reference genome of

*Gymnocypris eckloni* in GenBank (accession ID: JAMHKY000000000) (Wang et al., 2022) using HISAT2 (version 2.1.0). The DESeq R package (version 1.18.0) was used for differential expression analysis of RNAs between two groups. Genes exhibiting a false discovery rate (FDR) of  $<0.05$  and an absolute fold change value of  $\geq 2$  were identified as differentially expressed genes (DEGs). Subsequently, we mapped all DEGs to Gene Ontology (GO) database (<http://www.geneontology.org/>) and Kyoto Encyclopedia of Genes and Genomes (KEGG) database (<http://www.genome.jp/kegg/>) using the clusterProfiler R package. P-values were adjusted using the Bonferroni correction method. GO terms and KEGG pathways with corrected P-values of  $<0.05$  were considered significantly enriched by DEGs.

### 2.8. Metabolomic analysis

Liver tissues (approximately 80 mg) were sectioned on dry ice and collected in an Eppendorf tube (2 mL). After the tissues were homogenized, a methanol–acetonitrile solution (1:1, v/v) was added for metabolite extraction. All samples were analyzed via LC-MS/MS, with each group comprising six biological replicates. Separation was achieved using a UHPLC system (1290 Infinity LC, Agilent Technologies), and the primary and secondary spectra of the samples were acquired using a quadrupole time-of-flight mass spectrometer (AB Sciex TripleTOF 6600). Raw data were converted to the MzML format using ProteoWizard and subsequently analyzed using the XCMS program for peak alignment, retention time correction, and peak area extraction. Metabolites were detected in both positive ion mode (POS) and negative ion mode (NEG). The ropls R package (<http://www.r-project.org/>) was used to implement orthogonal projections to latent structures-discriminant analysis (OPLS-DA) to compare two groups. Cross-validation and permutation tests were performed to validate the reliability of the OPLS-DA model. The variable importance in projection (VIP) score of the OPLS model was used to rank metabolites based on their ability to distinguish between two groups. Metabolites with P-values (t-test) of  $<0.05$  and VIP scores of  $\geq 1$  were considered to be differentially expressed between two groups. Based on the results of metabolite characterization, the corresponding compound IDs were obtained from the KEGG database. Pathways with a P-value of  $<0.05$  were considered to be significantly enriched by the differentially expressed metabolites.

### 2.9. Integrated transcriptomic and metabolomic analysis

Based on the results of transcriptomic and metabolomic analysis, an integrated analysis was performed using the OmicShare tools to compare the heat stress and control groups. Differentially expressed genes (DEGs) with a P-value of  $<0.05$  and significantly different metabolites (SDMs) with a VIP score of  $>1$  and P-value of  $<0.05$  were simultaneously mapped to the KEGG database to identify common pathways. Subsequently, specific and overlapping pathways in the two comparison groups were identified.

### 2.10. Validation of transcriptomic data via qRT-PCR

To validate the accuracy of the transcriptomic data, five DEGs from each group were selected for quantitative reverse transcription polymerase chain reaction (qRT-PCR). The selected genes and corresponding PCR primers are listed in Table S1. The total RNA used for qPCR was consistent with that used for RNA sequencing. First-strand cDNA was synthesized using HiScript III All-in-one RT SuperMix Perfect for qPCR (Vazyme, Nanjing, China), and qPCR was performed on the QuantStudio 3 Real-Time PCR System (Thermo Fisher, USA) using ChamQ Universal SYBR qPCR Master Mix (Vazyme, Nanjing, China) according to the manufacturers' protocols. All samples were analyzed in triplicate, including three technical replicates and three biological replicates. The relative RNA expression of target genes was calculated using the  $2^{-\Delta\Delta\text{Ct}}$  method, with  $\beta\text{-actin}$  serving as the internal reference (Livak and

Schmittgen, 2001).

### 2.11. Statistical analysis

The SPSS (version 26.0) software (SPSS Inc., USA) was used for data processing. All experimental data were expressed as the mean  $\pm$  SD. The Brown–Forsythe test (for assessing the homogeneity of variance), one-way analysis of variance (ANOVA), and Duncan’s multiple range test were performed to determine the significance of differences between the control and experimental groups. Statistical significance was denoted as follows: \*,  $P < 0.05$ ; \*\*,  $P < 0.01$ ; and \*\*\*,  $P < 0.001$ . Non-significant differences were denoted as “ns”. Graphs were generated using the GraphPad Prism (version 9.5) software (GraphPad Software Inc., CA, USA).

## 3. Results

### 3.1. Effects of acute and chronic heat stress on liver histopathology

The histopathological changes observed in the liver of *G. eckloni* under acute and chronic heat stress are demonstrated in Fig. 1. In the control group (Fig. 1A), the arrangement of liver cells appeared orderly and compact, with hepatic lobules and sinusoids arranged radially around the central vein. The cell boundaries were distinct; nuclei were large, round, and centrally located, exhibiting deep staining; and the overall structure of the cells appeared clear and exhibited normal morphology. However, liver tissues showed varying degrees of histological alterations in the AH and CH groups. In the CH group (Fig. 1B), liver tissues exhibited a scattered cell arrangement, with some nuclei deviating from their original position. Additionally, the gap between the hepatic sinusoids was increased, and blood cells and vacuoles became clearly visible. In the AH group (Fig. 1C and 1D), the transverse section of the central vein appeared irregularly shaped and had blood cell accumulation. Moreover, the liver tissues showed vacuolar degeneration, a fuzzy cell shape, nuclear pyknosis, nuclear lysis, and increased

blood cell infiltration.

### 3.2. Effects of acute and chronic heat stress on the ultrastructure of hepatic cells

In the control group, hepatic cells exhibited a normal ultrastructure (Fig. 2A–C). The nuclei were large, round, and centrally located within the cell, containing prominent nucleoli. The cell membranes appeared intact and clear. In addition, abundant and well-developed mitochondria and rough endoplasmic reticulum were observed. However, after exposure to heat stress, notable changes were observed in the hepatocytes of the CH group (Fig. 2D–F). Particularly, fat droplets began to accumulate in hepatocytes, accompanied by blurred cell membrane boundaries and dilated endoplasmic reticulum. In the AH group (Fig. 2G–I), hepatocytes showed an increased size and number of lipid droplets, some of which were larger than the nucleus. The excessive accumulation of lipid droplets led to atrophy or compression of the nucleus, resulting in its displacement toward the cell periphery. Mitochondria exhibited loss of cristae and matrix and structural damage to the membranes. Additionally, the rough endoplasmic reticulum was fragmented.

### 3.3. Apoptosis of liver cells under acute and chronic heat stress

After DAPI staining, the nuclei in the control group mostly appeared as individual dots and fluorescence signals of nuclear DNA were strong. However, after exposure to heat stress, the fluorescence signals became weak, the nuclei were fragmented, and the chromatin appeared agglomerated and marginalized. The number of TUNEL-positive cells (red fluorescence) was higher in the CH and AH groups, indicating that heat stress promoted liver cell apoptosis (Fig. 3A). Furthermore, the AH group exhibited the lowest cell viability, indicating the most severe injury (Fig. 3B).

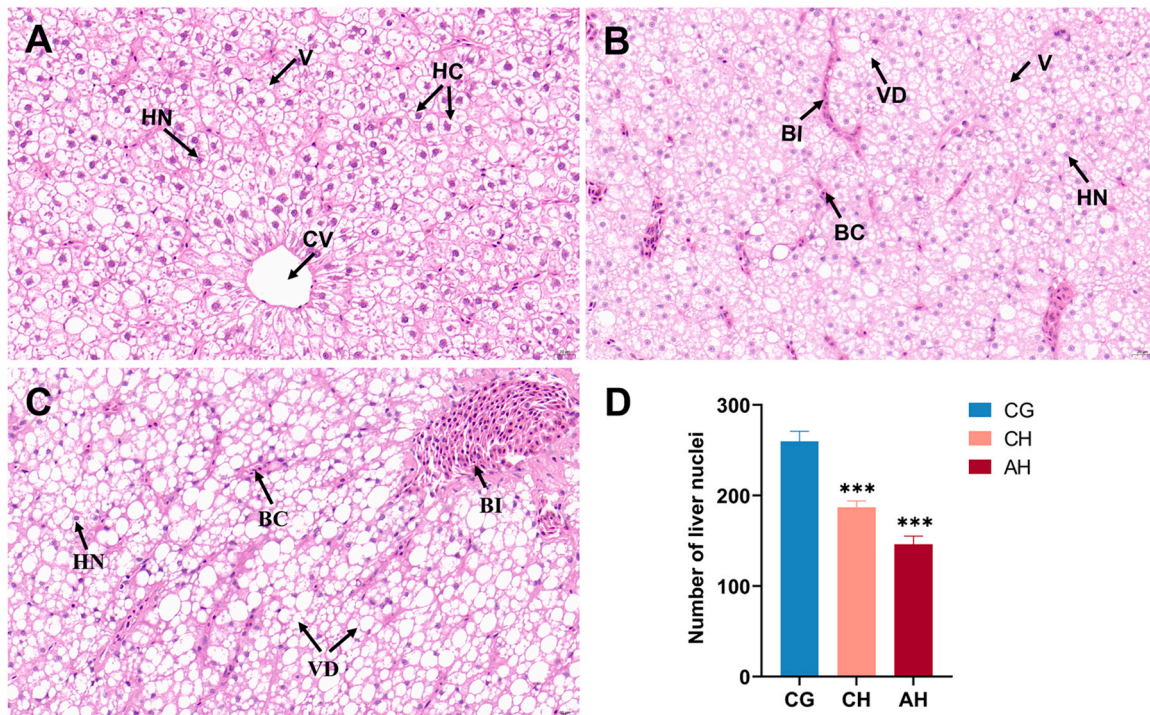


**Fig. 1.** Effects of acute and chronic heat stress on liver histopathology. A: CG group, B: CH group, C: AH group, D: Effects of heat stress on the number of nuclei in the liver of *G. eckloni*. HC, hepatic cell; HN, hepatic nucleus; V, vacuole; CV, central vein; BC, blood cell; VD, vacuolar degeneration; BI, blood cell infiltration. Scale bar = 20  $\mu$ m.

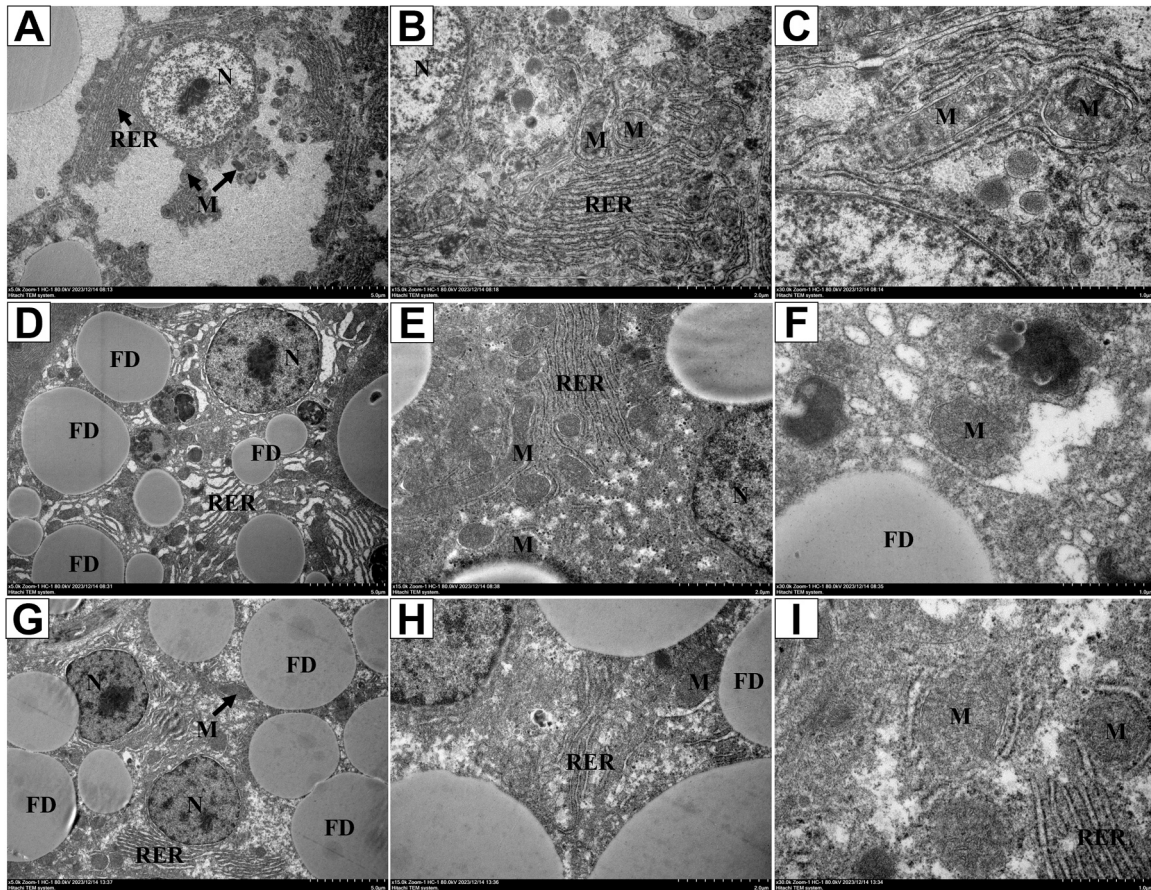


**Fig. 2.** Transmission electron microscope (TEM) images of the ultrastructure of hepatic cells under acute and chronic heat stress. A, B, C: Control group; D, E, F: CH group; G, H, I: AH group. M, mitochondria; N, nucleus; RER, rough endoplasmic reticulum; FD, fat droplet. A, D, G: scale bars = 5.0  $\mu\text{m}$ ; B, E and H: scale bars = 2.0  $\mu\text{m}$ ; C, F and I: scale bars = 1.0  $\mu\text{m}$ .

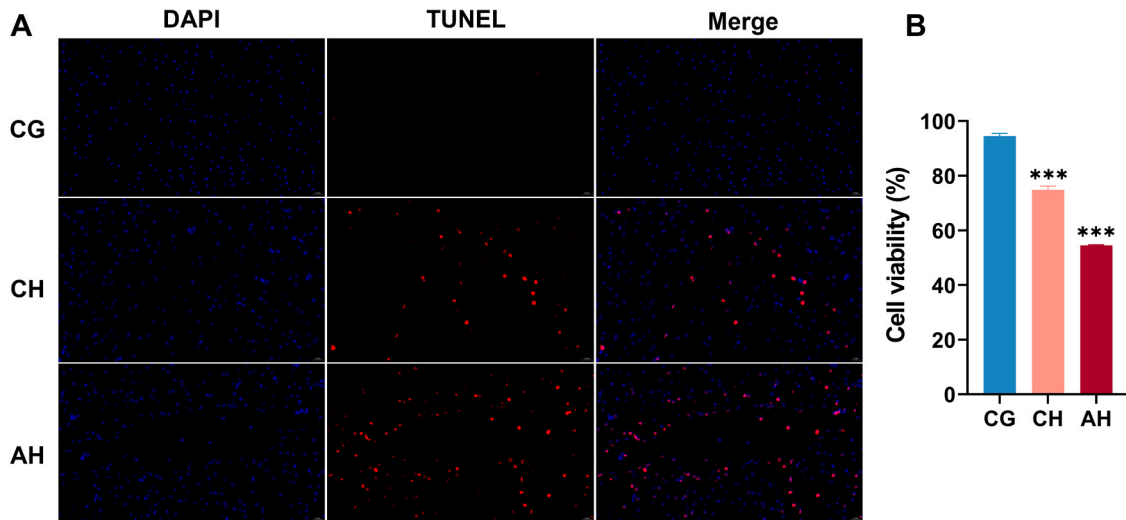


**Fig. 3.** Apoptosis of liver cells after acute and chronic heat stress. A: Liver tissues stained with 4',6-diamidino-2-phenylindole (DAPI) and terminal deoxynucleotidyl transferase deoxy-UTP nick-end labeling (TUNEL). B: Cell viability in the control and heat-stress groups.

**3.4. Effects of acute and chronic heat stress on biochemical indices**

Fig. 4 shows the changes in serum and liver biochemical indices in *G. eckloni* under acute and chronic heat stress. The serum levels of ALT and AST were higher in the CH and AH groups than in the control group ( $P < 0.01$ ). Glucose levels were significantly higher in the AH group ( $P <$

0.05), with no significant changes being observed in the CH group. In addition, cortisol levels were significantly higher in the CH ( $P < 0.05$ ) and AH ( $P < 0.01$ ) groups (Fig. 4A).

With regard to hepatic oxidative stress indicators (Fig. 4B), the levels of ROS and MDA were significantly higher in the CH and AH groups than in the control group ( $P < 0.05$  for ROS;  $P < 0.01$  for MDA). CAT activity

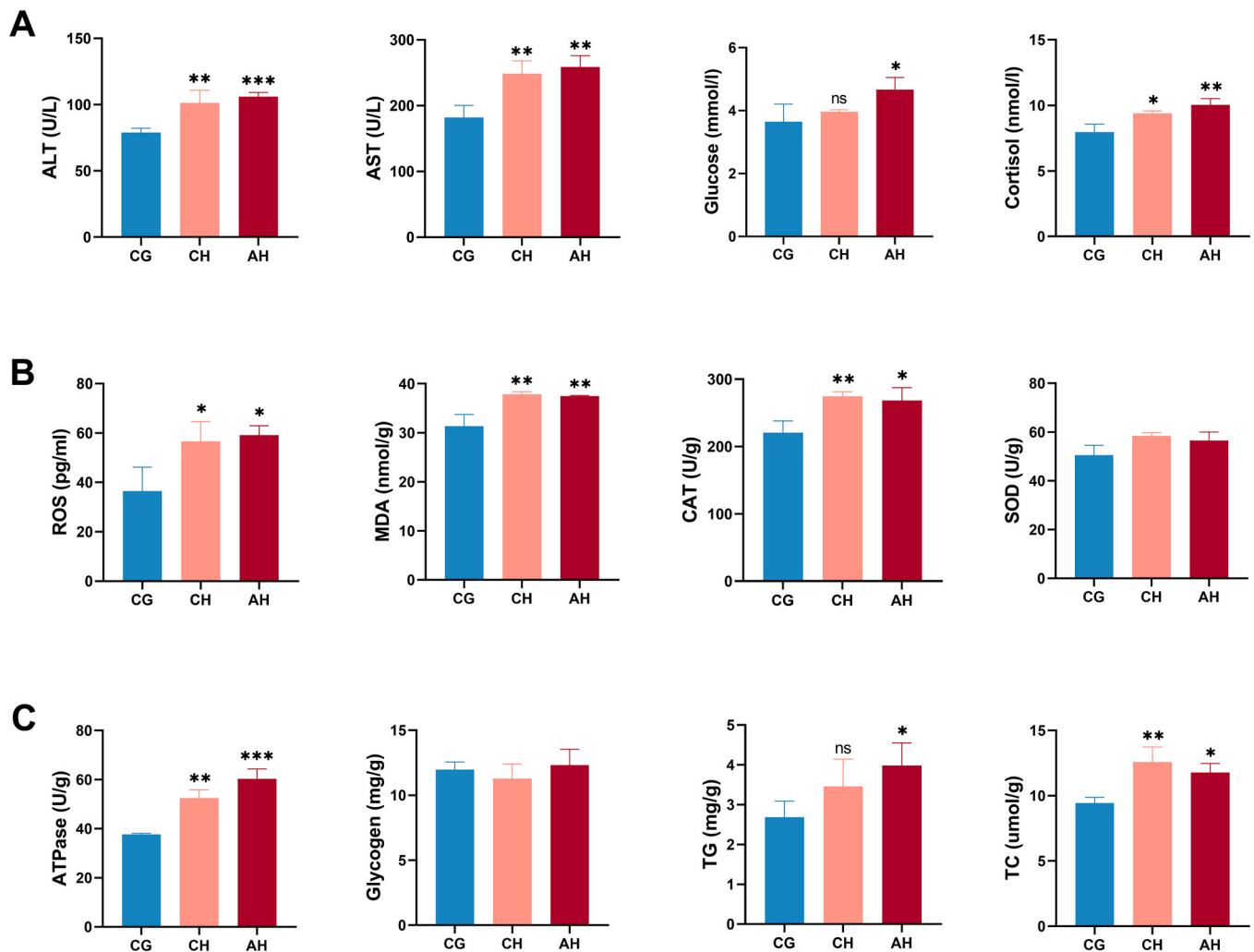


**Fig. 4.** Effects of acute and chronic heat stress on biochemical indices. A represents the changes in serum biochemical indices; B represents the changes in hepatic oxidative stress indicators; C represents the changes in hepatic energy metabolism indicators.

significantly increased in response to both acute and chronic heat stresses ( $P < 0.05$ ), whereas SOD activity remained unchanged following heat stress.

With regard to energy metabolism indicators (Fig. 4C), the levels of ATPase and TC significantly increased in response to both acute and chronic heat stresses ( $P < 0.01$ ). TG levels were significantly higher in the AH group; however, no significant changes were observed in the CH group. Additionally, glycogen content did not show significant changes in response to acute or chronic heat stress.

### 3.5. Transcriptomic analysis of *G. eckloni* liver under acute and chronic heat stress

To identify genes associated with the response to acute and chronic heat stress, RNA sequencing (RNA-seq) was performed on liver tissue samples from the CG, CH, and AH groups, each with three biological replicates. The results revealed approximately 33.38–57.22-Mb raw reads. After quality-control analysis based on Q20 and Q30 scores, 33.02–57.07 million clean reads were obtained in each sample (Table S2). All raw sequences have been uploaded to the NCBI database under the accession number PRJNA1091806.

Differential expression analysis revealed a total of 2083 DEGs, with 1011 downregulated and 1072 upregulated genes, between the CG and CH groups (Fig. 5A). Similarly, a total of 2878 DEGs, with 1564 downregulated and 1314 upregulated genes, were identified between the CG

and AH groups (Fig. 5B). As shown in the Venn diagram and heatmap in Fig. 5C and 5D, respectively, 937 genes were common between the two DEG sets.

The DEGs in the CG versus CH group were enriched in 540 GO terms, including 275 terms related to biological processes (BPs), 175 terms related to molecular functions (MFs), and 90 terms related to cellular components (CCs) (Fig. S1). The significantly enriched GO terms included “tetrapyrrole binding;” “heme binding;” “oxidoreductase activity;” “catalytic activity;” “unfolded protein binding;” and “oxidoreductase activity, acting on paired donors, with incorporation or reduction of molecular oxygen”. Similarly, the DEGs in the CG versus AH group were enriched in 335 GO terms, including 169 terms related to BPs, 112 terms related to MFs, and 54 terms related to CCs (Fig. S1). The significantly enriched GO terms included “organonitrogen compound metabolic process;” “nucleoside metabolic process;” “glycosyl compound metabolic process;” and “small molecule metabolic process” (Fig. 6A).

The top 10 significant KEGG pathways associated with the DEGs are shown in Fig. 6B, and detailed information ( $q < 0.05$ ) is provided in Table S3. KEGG enrichment analysis demonstrated that the DEGs in the CG versus CH group were significantly enriched in pathways such as metabolic pathways, protein processing in the endoplasmic reticulum, tryptophan metabolism, pyruvate metabolism, glycolysis/gluconeogenesis, fat digestion and absorption, and cholesterol metabolism. Conversely, the DEGs in the CG versus AH group were significantly

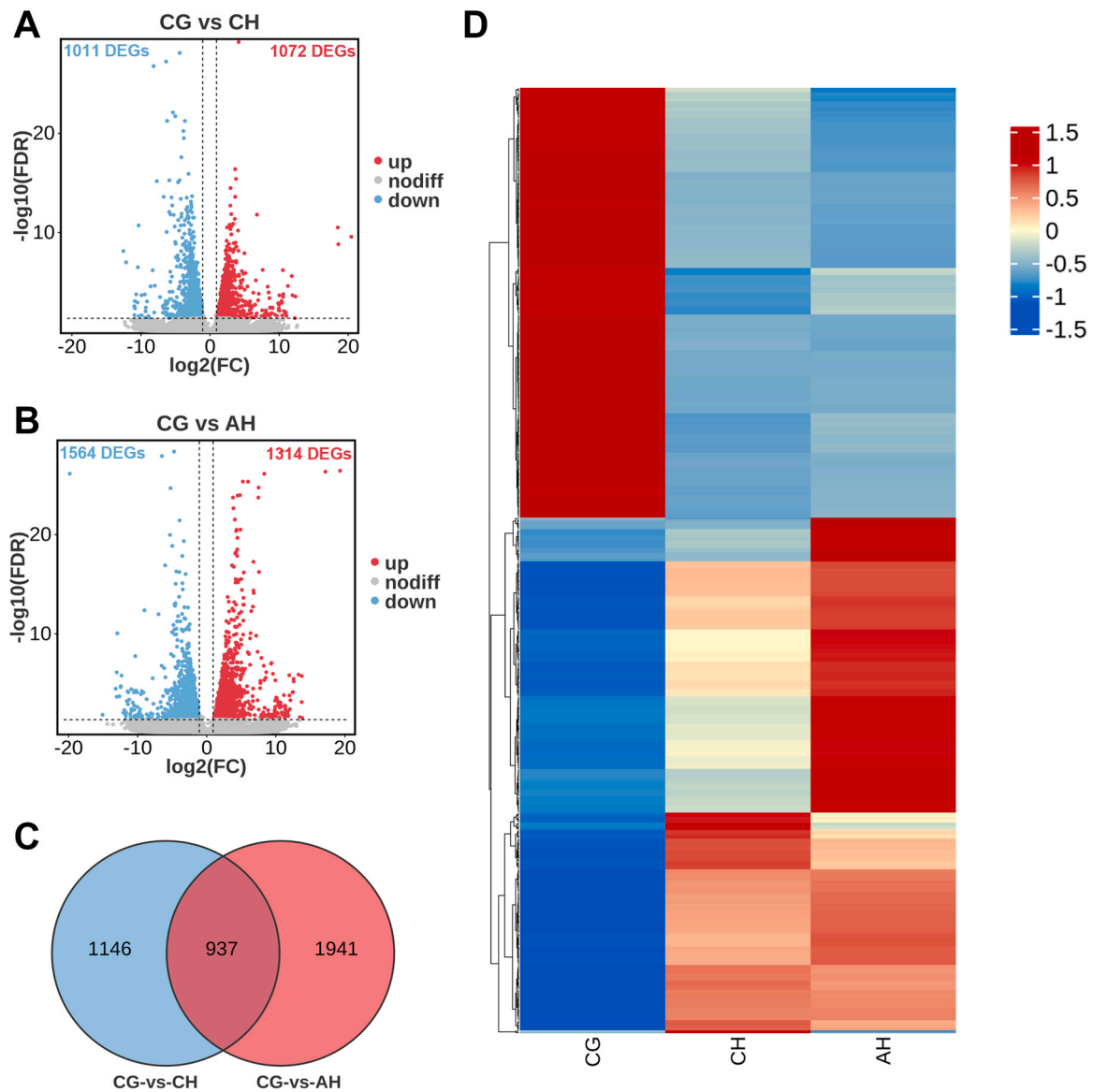


**Fig. 5.** Distribution of DEGs in the liver of *G. eckloni* under acute and chronic heat stress. A, B: Volcano maps of the DEGs between the CG and CH groups and between the CG and AH groups. Each dot represents a gene, with red indicating significantly upregulated genes, blue indicating significantly downregulated genes, and gray representing non-significant differentially expressed genes. C, D: Venn diagram and heatmap of the overlapping genes between the two DEG sets.

enriched in pathways such as glycolysis/gluconeogenesis, carbon metabolism, HIF-1 signaling pathway, protein processing in the endoplasmic reticulum, and the pentose phosphate pathway. Notably, both DEG sets were significantly enriched in the protein processing in the endoplasmic reticulum pathway. To examine the regulatory mechanism of this pathway, the expression profiles of genes involved in the pathway were selected for further investigation (Fig. 7).

In particular, *uggt1*, *pdia3*, *hsp70*, *fabp7*, and *tfrc* genes from the CG versus CH group and *hsp90aa1*, *egln*, *pck1*, *man1b1*, and *atf4* genes from the CG versus AH group were validated via qRT-PCR. The results exhibited a high degree of consistency with those of RNA-seq analysis (Fig. 6C), indicating the reliability and validity of the transcriptomic data.

### 3.6. Metabolomic analysis of *G. eckloni* liver under acute and chronic heat stress

Non-targeted metabolomic analysis was performed to investigate metabolic changes in the liver of *G. eckloni* in the CG, CH, and AH

groups. A total of 3037 metabolites were detected in 18 liver samples from the three groups (six replicates per group), with 1750 and 1287 metabolites being detected in the positive (POS) and negative (NEG) ion modes, respectively. An OPLS-DA model was used to identify and visualize differentially expressed POS-ion-mode-detected metabolites between the control and experimental groups. The score plot demonstrated that the model could distinguish between the control group and the two experimental groups (Fig. 8A and B), revealing significant differences in metabolic profiles between the groups. Validation of the model, including a replacement test with  $n = 200$ , indicated low Q2 intercept values, suggesting the reliability and effectiveness of the OPLS-DA model (Fig. 8C and D).

Based on OPLS-DA analysis, metabolites with a  $P$ -value of  $< 0.05$  and VIP score of  $\geq 1$  were considered to be differentially expressed. Specifically, a total of 180 differentially expressed metabolites (67 upregulated and 113 downregulated) were identified between the CG and CH groups, whereas a total of 242 differentially expressed metabolites (37 upregulated and 205 downregulated) were identified between the CG and AH groups (Fig. 8A and B). A majority of these metabolites were

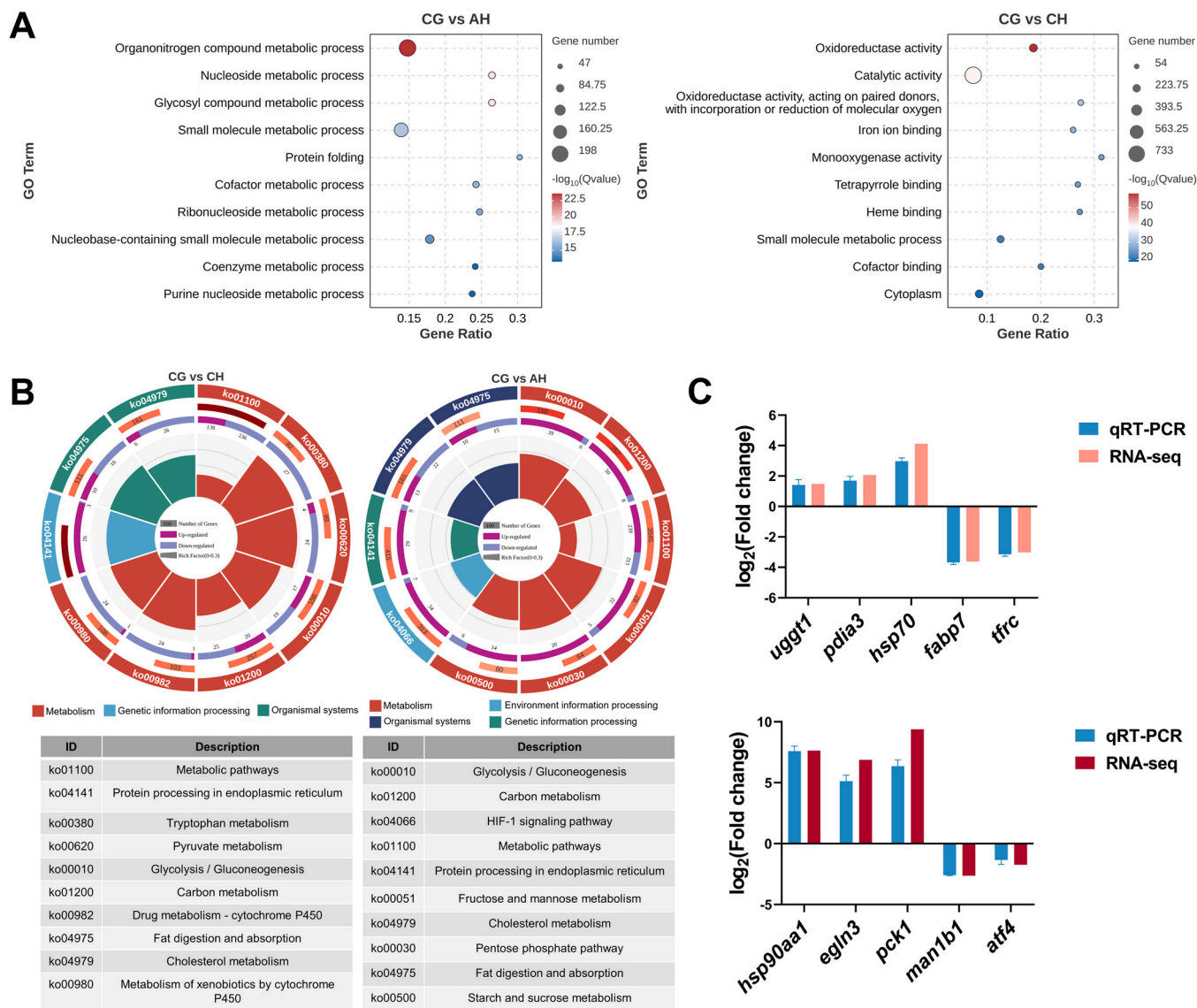


**Fig. 6.** GO and KEGG enrichment analyses of the two DEG sets. A: Bubble diagram of the top 10 significantly enriched GO terms. B: Circle diagram of the top 10 significantly enriched KEGG pathways. C: Comparison of gene expression levels determined via qRT-PCR and RNA-seq.

classified as organic acids and derivatives, lipids and lipid-like molecules, organoheterocyclic compounds, and benzenoids (Fig. 9C). A total of 85 metabolites were common between the two metabolite sets (Fig. 9D).

KEGG pathway enrichment analysis of the two differentially expressed metabolite sets revealed similar results, with the metabolites being predominantly enriched in pathways related to metabolism (including global and overview maps, amino acid metabolism, chemical structure transformation maps, and lipid metabolism), organismal systems (including the digestive system, nervous system, and endocrine system), and environmental information processing (including membrane transport) (Fig. S2). However, only a few significantly enriched pathways ( $P < 0.05$ ) were identified for both metabolite sets. The differential metabolites in the CG versus CH group were significantly enriched in pathways such as tryptophan metabolism and bile secretion, whereas those in the CG versus AH group were significantly enriched in pathways such as biosynthesis of alkaloids derived from the shikimate pathway, ether lipid metabolism, and steroid hormone biosynthesis (Figs. 9E and 9F).

### 3.7. Integrated metabolomic and transcriptomic analysis of *G. eckloni* liver tissues under acute and chronic heat stress

The DEGs and differential metabolites (POS) identified in the CG versus CH group and the CG versus AH group were mapped to the KEGG database to identify common pathways affected by heat stress. The results showed that the aforementioned DEGs and differential metabolites (POS) were enriched in 49 and 72 pathways, respectively; of which, 35 and 48 pathways were related to metabolism, respectively. These results indicated that heat stress had a profound impact on the metabolic activity of *G. eckloni* liver. KEGG pathways that were significantly associated ( $P < 0.05$ ) with at least one omic gene set were selected from the CG versus CH group and the CG versus AH group, resulting in 27 and 24 pathways, respectively (Fig. 10A and B). A Venn diagram was generated to visualize specific and overlapping pathways related to metabolism in the CG versus CH group and the CG versus AH group (Fig. 10C). A total of 11 overlapping pathways were identified, mainly including those related to carbohydrate metabolism, lipid metabolism and, global and overview maps. A total of 13 pathways specific to the CG versus CH group were identified. These pathways were mostly related to amino acid metabolism, with tryptophan metabolism being significantly



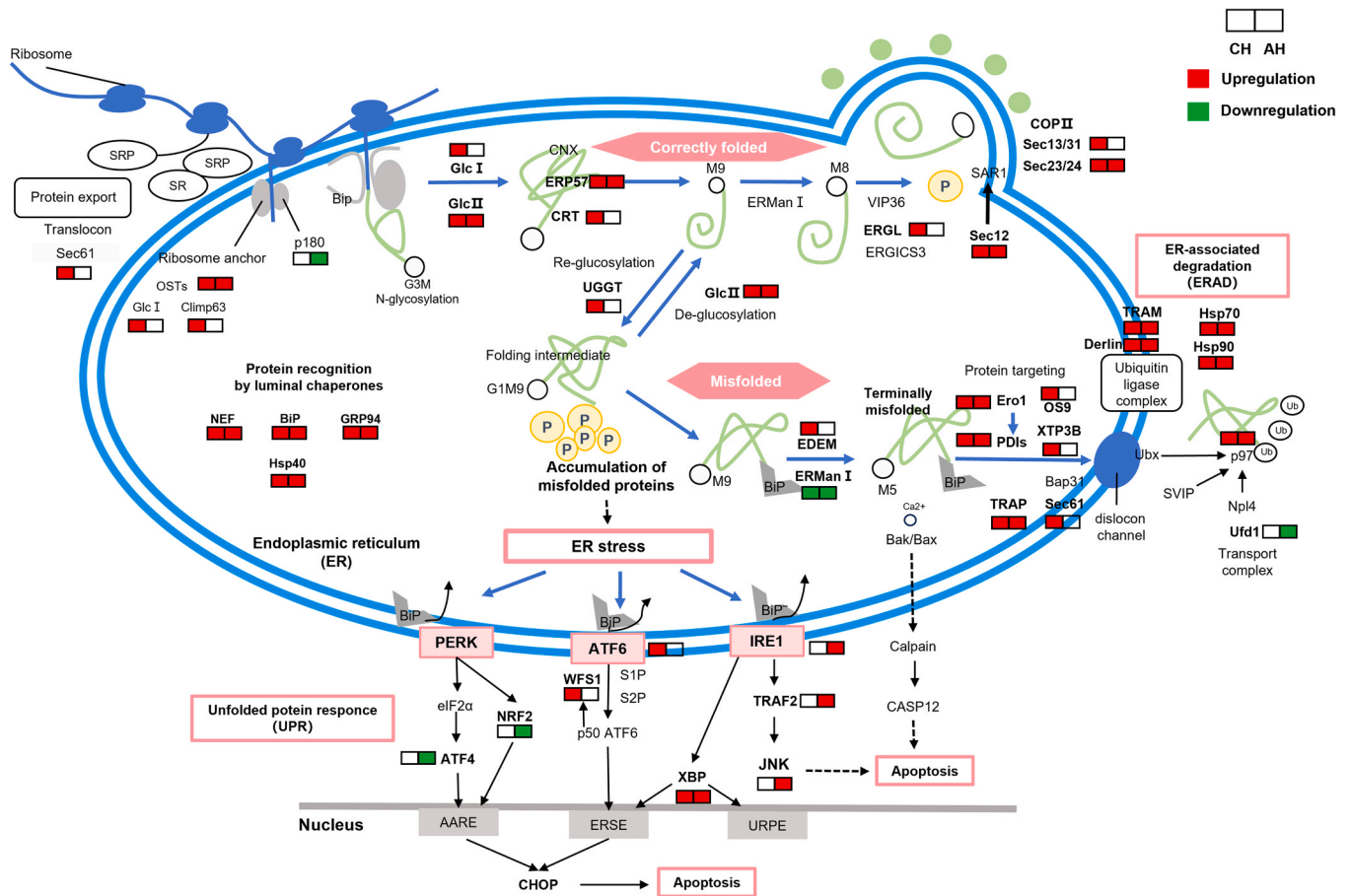


Fig. 7. Mechanism of the protein processing in endoplasmic reticulum pathway in response to acute and chronic heat stress.

enriched by both the differential metabolites and DEGs. A total of 7 pathways specific to the CG versus AH group were identified, which were primarily related to lipid metabolism, including fatty acid biosynthesis, arachidonic acid metabolism, and ether lipid metabolism. Further investigation into the regulatory mechanisms of the tryptophan metabolic pathway (Fig. 11) revealed that the *ido*, *tdo*, *aoc1*, *aldh*, *hao*, and *acmsd* genes were downregulated in response to heat stress. In addition, the levels of L-tryptophan, xanthurenic acid, indole-3-ylacetonitrile, and indole-3- acetamide significantly increased and those of acetyl coenzyme A (acetyl-CoA) decreased in response to heat stress.

#### 4. Discussion

High temperatures significantly affect the growth of economically important cold-water fish species, with heat stress emerging as a substantial threat to the cultivation of *G. eckloni*. The increasing temperatures during summer and the prevalence of extreme climate events increase the risk of heat stress. The liver, adept at modulating metabolic processes, serves as an important organ for studying the mechanisms underlying heat adaptation. In this study, we investigated the effects of chronic and acute heat stress on the liver of *G. eckloni* by assessing serum and hepatic biochemical indices, histopathological features of the liver, and the transcriptomic and metabolomic profiles of the liver. The findings provided valuable insights into the mechanisms underlying the adaptive response of *G. eckloni* to heat stress.

##### 4.1. Liver tissue damage under heat stress

High temperatures can cause structural changes in or damage to

tissues or organs, impacting their functionality (Wang et al., 2019). Histopathology enables rapid detection of morphological changes in tissue structures (Wolf et al., 2015). Liver tissue damage, characterized by hemocyte infiltration and extensive vacuolization, has been observed in *Hypophthalmichthys nobilis* and *Pelteobagrus fulvidraco* after exposure to heat stress (Lin et al., 2018; Wang et al., 2024). Similarly, this study showed that heat stress caused liver tissue damage, characterized by significant lipid droplet accumulation, mitochondrial structural abnormalities, and endoplasmic reticulum fragmentation in hepatocytes, in *G. eckloni*. These findings are consistent with those of a study that correlated such morphological changes with oxidative stress in *Micropterus salmoides* (Zhao et al., 2022). Notably, histopathological and morphological analyses demonstrated more severe damage in the AH group, which is consistent with the results of a study on *Paralichthys olivaceus* (Han et al., 2023). Activation of the mitochondrial apoptotic pathway during acute heat stress suggests the presence of a vicious cycle between oxidative stress and inflammation, which exacerbates liver injury (E. Liu et al., 2022). In this study, TUNEL analysis revealed a significant increase in the number of apoptotic cells in response to heat stress. In particular, the viability of hepatocytes was substantially lower in the AH group, validating the increased severity of liver injury caused by acute heat stress. ALT and AST are crucial indicators of liver function; their increased levels indicate impaired liver function (Liu et al., 2022). Consistently, we found significantly increased serum levels of ALT and AST after heat stress, particularly in the AH group. This increase preliminary indicates liver dysfunction, which may impact amino acid metabolism (Li et al., 2023).

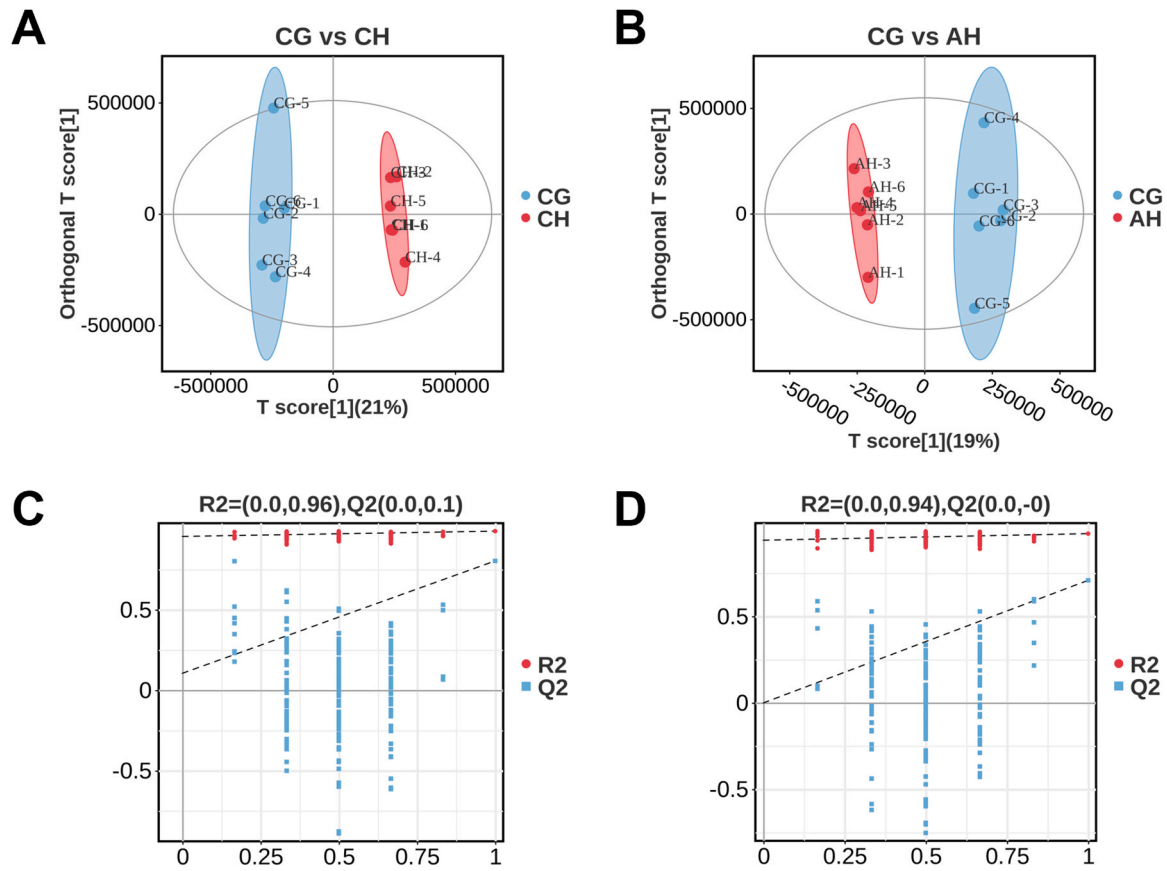


**Fig. 8.** Score plots of OPLS-DA analysis of *G. eckloni* liver metabolites under normal and heat stress conditions. A and B: Substitution test plots of OPLS-DA analysis for the CG versus CH group and the CG versus AH group. C and D: Corresponding validation plots of OPLS-DA model.

#### 4.2. Oxidative stress and physiological metabolism under heat stress

When fish are exposed to high temperatures, their aerobic metabolism is stimulated, leading to the production and accumulation of ROS and free radicals, which result in oxidative stress (Wang et al., 2023). Oxidative stress triggers the activation of the antioxidant defense system, enhancing antioxidant capacity and maintaining homeostasis, especially through antioxidant enzymes (Langston et al., 2002). This study showed that the liver of *G. eckloni* produced large amounts of ROS under heat stress. The significant increase in CAT activity, but not in SOD activity, may be attributed to the species-specific response of antioxidant enzymes to heat stress (Lu et al., 2016). These findings suggest that under heat stress, the liver of *G. eckloni* protects cells against ROS-induced damage by increasing CAT activity, thereby converting  $H_2O_2$  to water and oxygen (Langston et al., 2002). However, when excess ROS are produced, they interact with membrane lipids, causing membrane lipid peroxidation, the content of MDA reflects the intensity of oxidative damage (Zhou et al., 2023). In this study, MDA levels were significantly higher in both the CH and AH groups, indicating that free radicals caused considerable oxidative damage to liver cells. The limited ability of liver cells to regulate their antioxidant defenses renders them unable to counteract excess oxygen free radicals and lipid peroxides, eventually leading to cellular damage or apoptosis (Kaur et al., 2005). These findings are consistent with the changes observed in the ultrastructure of hepatocytes in *G. eckloni* exposed to heat stress.

As external environmental pressures intensify, they disrupt the balance of energy allocation in the body, leading to increased energy consumption to resist stresses (Sokolova et al., 2012). Moderate increases in cortisol levels following heat stress, as observed in species such as *Oncorhynchus mykiss* (Lu et al., 2022) and *Megalobrama amblycephala* (Li et al., 2019), promote hepatic gluconeogenesis and

glycogenolysis, increasing the concentration of glucose to meet the energy demands augmented by heat stress (Long et al., 2023). This study showed an increase in the serum levels of cortisol and glucose following heat stress, suggesting the body's ability to combat environmental stress by increasing serum glucose levels. In addition, the higher levels of TGs and TC in the CH and AH groups than in the control group suggest that lipid catabolism is downregulated in response to heat stress to meet the increased energy demands, a phenomenon that has been observed in *Paralichthys olivaceus* (Han et al., 2023). ATPase, a more accurate indicator of changes in energy metabolism (Li et al., 2019), exhibited a significant increase in both the AH and CH groups, validating that heat stress increased energy demands in the liver of *G. eckloni*. Furthermore, the levels of cortisol, glucose, ATPase, and TG were higher in the AH group than in the CH group, preliminarily suggesting that *G. eckloni* experienced more severe damage and required more energy during acute heat stress than during chronic heat stress under similar temperature conditions.

#### 4.3. Transcriptomic response to heat stress in the liver

Transcriptomic analysis revealed that DEGs in the CG versus CH group and the CG versus AH group were significantly enriched in the "protein processing in the endoplasmic reticulum" pathway. In the endoplasmic reticulum (ER), a quality-control system comprising calnexin (CNX), calreticulin (CRT), and their associated chaperone ERp57 ensures proper protein folding (Gupta, 2012). Misfolded proteins generated under stress are recognized by luminal chaperones and subsequently transported to the ER membrane for ER-associated degradation (ERAD) (Plemper et al., 1997). In this study, the post-stress increase observed in *pdia3* or *calr* expression in the liver of *G. eckloni* suggests that correct protein folding was ensured. However, the post-stress increase

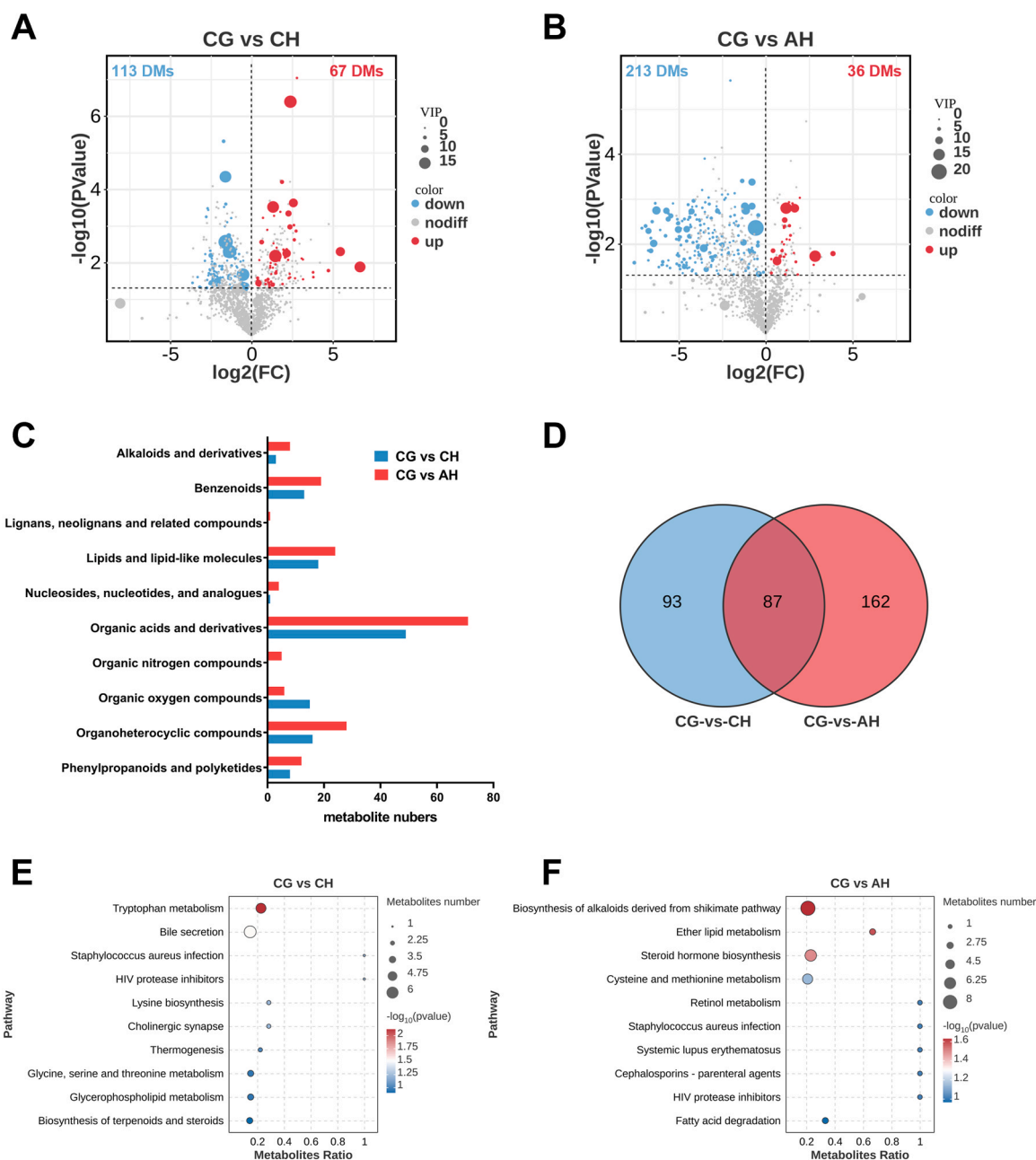


**Fig. 9.** Differential metabolites (POS) and KEGG enrichment analysis. A, B: Volcano plots demonstrating the distribution of differential metabolites between the CG and CH groups and between the CG and AH groups. C: Classification of the two differential metabolite sets. D: Venn diagram demonstrating the overlap between the two differential metabolite sets. E and F: Top 10 KEGG pathways in the CG versus CH group and the CG versus AH group.

observed in the expression of luminal chaperone genes, such as *hyou1*, *hspa5*, *hsp90b*, *dnajb11*, *dnajc1*, *dnajc10*, and *scj1*, indicates the accumulation of misfolded proteins in the ER, leading to ER stress. Heat shock proteins (HSPs) play a crucial role in ERAD. In most fish species, HSP70 and HSP90 are core proteins involved in the response to heat stress. These proteins are significantly induced in ERAD to enhance ubiquitin-dependent degradation and protect organisms from heat shock (Mahanty et al., 2017). In this study, the increase observed in the expression of *hspa1s* and *hsp90a* suggests that these proteins were over-activated to alleviate heat stress-induced damage in the liver of *G. eckloni*. Furthermore, the increase observed in the expression of *ero1l*, *ero1lb*, *pdia1*, *pdia4*, and *pdia6* indicates an increase in catalytic oxidative protein folding and maintenance of ER redox homeostasis, which has been observed in other fish species, such as *Micropterus salmoides* and *Larimichthys polyactis* (Liu et al., 2023; Zhao et al., 2022).

When the amount of misfolded proteins in the ER exceeds the capacity for recovery, it can trigger the unfolded protein response (UPR), potentially leading to apoptosis. The UPR involves three pathways, namely, IRE1, PEPK, and ATF6 (Choi et al., 2010). This study showed differential activation of UPR in the liver of *G. eckloni* under two types of heat stresses. Under chronic heat stress, upregulation of *atf6a*, *atf6b*, and *wfs1* in the ATF6 pathway and that of *xbp1* in the IRE1 pathway indicated that these pathways were activated to alleviate ER stress by clearing unfolded or misfolded proteins (Hetz et al., 2020). However, under acute heat stress, upregulation of *ern1*, *traf2*, and *jnk* in the IRE1 pathway suggested that IRE1 and its downstream JNK pathway were activated to promote apoptosis in the liver of *G. eckloni*. Additionally, downregulation of *nfe2l2* and *atf4* in the PEPK pathway indicated pathway inhibition, resulting in a shift from adaptive regulation to injury under acute heat stress (Braakman and Hebert, 2013). Therefore,

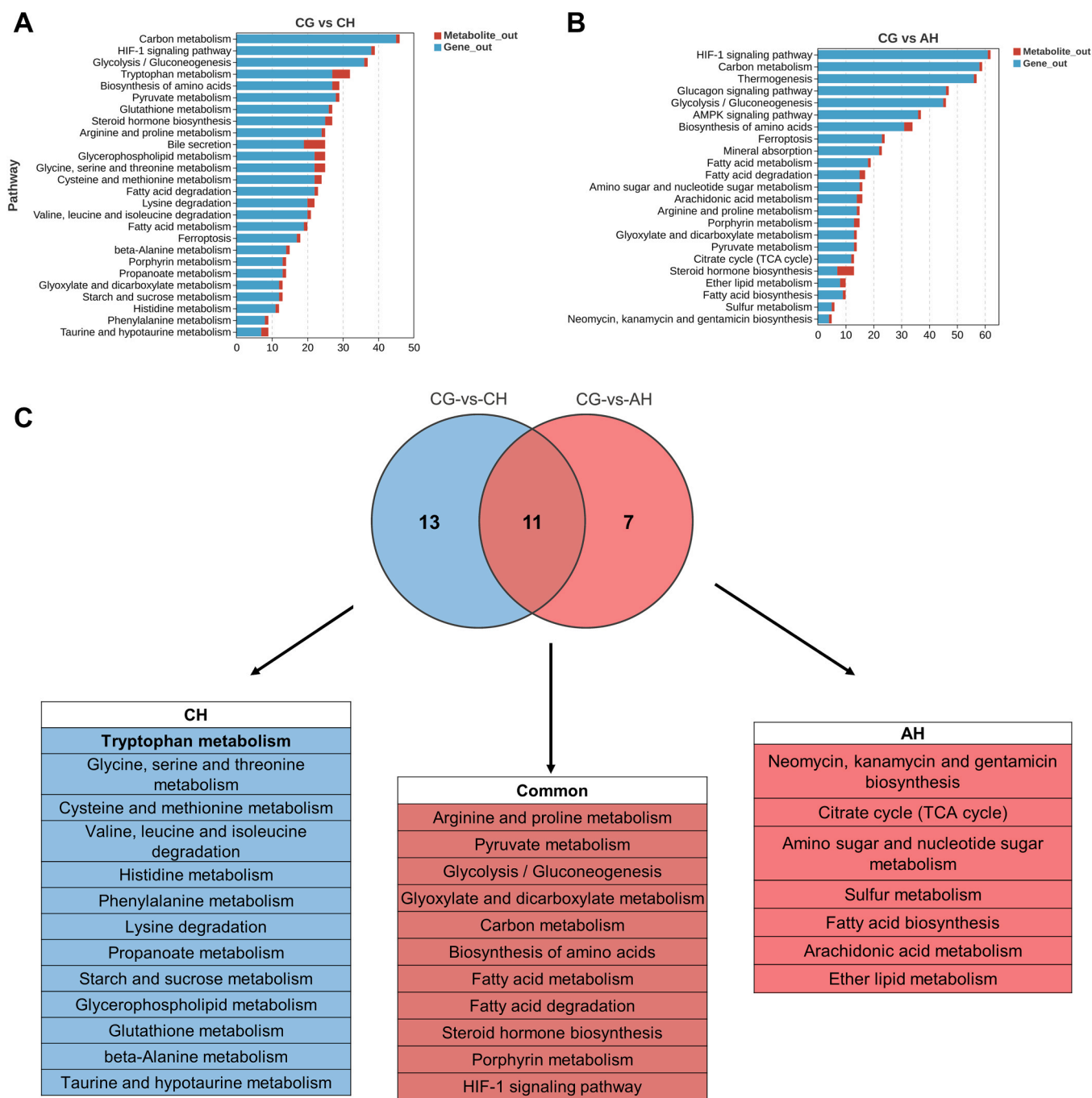


**Fig. 10.** Integrated metabolomic and transcriptomic analysis of *G. eckloni* liver tissues under normal and heat-stress conditions. A and B: Co-annotated KEGG pathways that were significantly associated with either the differential metabolites or the DEGs in the CG versus CH group and the CG versus AH group. C: Venn diagram of specific and overlapping pathways related to metabolism in the CG versus CH group and the CG versus AH group.

we hypothesize that IRE1–JNK may be the key pathway driving increased apoptosis of hepatocytes in *G. eckloni* under acute heat stress. A similar apoptotic mechanism has been observed in the hepatocytes of *Paralichthys olivaceus* under heat stress (Han et al., 2023).

#### 4.4. Metabolic response to heat stress in the liver

The categorization of differential metabolites and KEGG pathway enrichment analysis of these metabolites suggested that amino acid metabolism and lipid metabolism in the liver of *G. eckloni* play an important role in the response to heat stress. Amino acids serve as the building blocks of proteins and are essential for stress response (Wang

et al., 2022). In the CH group, several free amino acids and their derivatives, including cysteic acid, leucine, glutamic acid, histidine, and L-citrulline, were upregulated in the liver of *G. eckloni*. As discussed in the previous section, this upregulation may be associated with the degradation of misfolded proteins. Similarly, enhanced ubiquitin-dependent protein hydrolysis has been reported to increase amino acid levels in fish living at high altitudes, such as *Triplophysa siluroides* (Chen et al., 2023b). Creatine, contributing to ATP synthesis, serves as an important indicator of proteolysis (Qaid and Al-Garadi, 2021). This study showed an increase in creatinine levels in the liver of *G. eckloni* under heat stress, suggesting enhanced protein catabolism. Similar findings have been reported in a study on *Acipenser dabryanus*

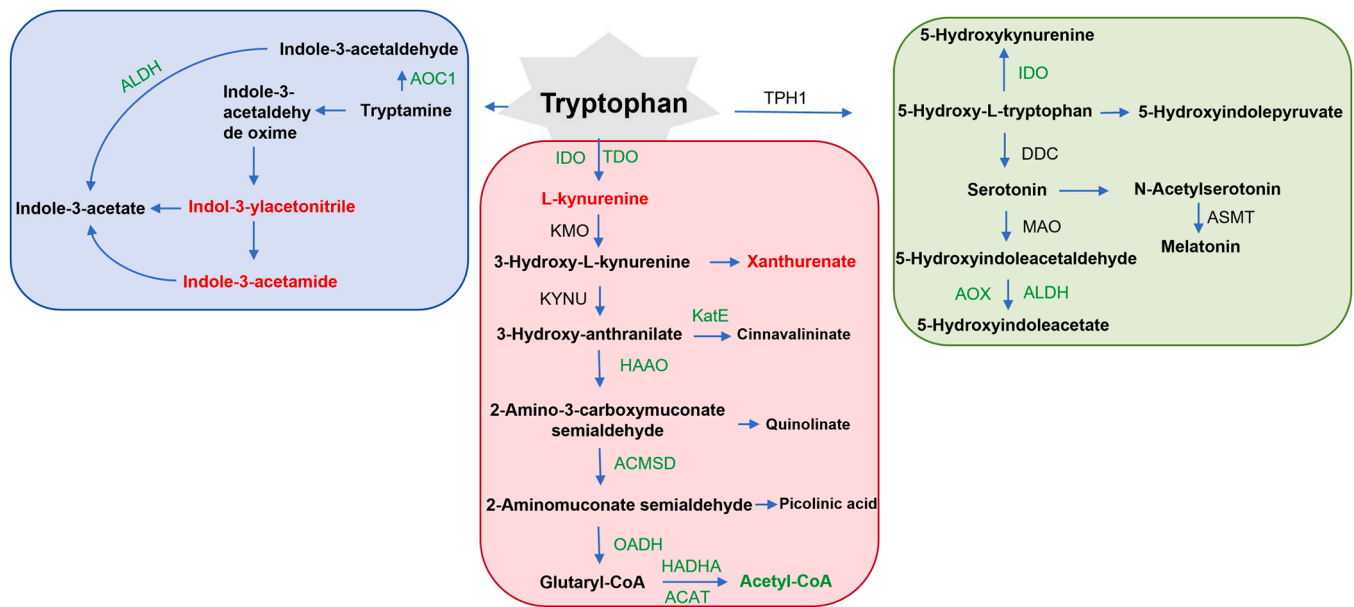


Fig. 11. Changes in DEGs and differential metabolites in the tryptophan metabolic pathway in response to chronic heat stress. Green represents downregulation of gene expression or a decrease in metabolite levels, and red represents upregulation of gene expression or an increase in metabolite levels.

(Chen et al., 2023a). Furthermore, amino acids can also serve as direct energy sources, promoting energy generation and providing additional energy to meet increased demands under severe conditions (Lu et al., 2017). In this study, the reduction observed in the levels of various organic acids and derivatives in the AH group, such as imazamox, methionine, glycine, and phenylalanine, suggests that these compounds are used as oxidizable amino acids to compensate for energy metabolism under severe heat stress conditions. Energy depletion may lead to a decrease in the levels of certain amino acids (Chen et al., 2022), a phenomenon that has been observed in *Scophthalmus maximus* (Yang et al., 2020).

Lipids serve as the primary energy substrates in organisms, and regulation of lipid metabolism is essential for maintaining homeostasis in response to external stimuli and stress (Su et al., 2021). Glycerophospholipids, major components of biological membranes, play an important role in maintaining cell membrane stability and mitigating cellular damage (Holmsen et al., 1992). In this study, the decrease observed in the levels of glycerophosphoethanolamine, glycerophosphocholine, and choline in response to heat stress suggests changes in the structure and function of the cell membrane of *G. eckloni*, which may impact membrane fluidity (Chen et al., 2022). A study showed that this downregulation might represent a mechanism to prevent the entry of ROS into cells and alleviate oxidative stress (Melvin et al., 2019). Additionally, the decrease observed in acetyl-CoA levels after heat stress may be associated with downregulation of lipolysis. Lipolysis involves the degradation of fatty acids to acetyl-CoA via the  $\beta$ -oxidation pathway in the peroxisome (Hou et al., 2016; Zhang et al., 2023; Zhao et al., 2024). In addition, acetyl-CoA serves as an important intermediate metabolite in energy metabolism, maintaining the balance between energy supply and demand (Jing et al., 2023). A decrease in acetyl-CoA levels may also be attributed to increased energy demands under stress, leading to amino acid and lipid mobilization (Costabile et al., 2022). Overall, the hepatic metabolic responses of *G. eckloni* to high temperatures are complex, involving mechanisms that alleviate oxidative stress and promote energy generation to meet increased demands by regulating amino acid and lipid metabolism.

#### 4.5. Effective pathways involved in the response to chronic heat stress in *G. eckloni*

Integrated metabolomic and transcriptomic analysis revealed that differential metabolites and DEGs in the “CG versus CH” group and the “CG versus AH” group were enriched in many overlapping or specific pathways. In particular, tryptophan metabolism was the only specific pathway significantly enriched by both the differential metabolites and DEGs in the CG versus CH group ( $p < 0.05$ ). Tryptophan, the sole amino acid derived from the indole group, participates in regulating various physiological functions, including inflammation, oxidative stress, metabolism, and immune responses (Sahu et al., 2020). Studies have shown that tryptophan is involved in the synthesis of proteins and nucleic acids and can regulate protein deposition and metabolism in fish liver (Zhang et al., 2022). Additionally, dietary supplementation of tryptophan has been demonstrated to reduce stress and improve health in *Gadus morhua* (Herrera et al., 2017). The main pathways involved in tryptophan metabolism include the kynurenine (Kyn), 5-hydroxytryptamine (5-HT), and indole pathways, with Kyn being the most important pathway and primarily occurring in the liver (Xue et al., 2023). In the Kyn pathway, tryptophan is converted to various metabolites, such as kynurenine, xanthurenic acid, kynurenic acid, and nicotinamide adenine dinucleotide (NAD<sup>+</sup>), which are involved in numerous metabolic reactions (Badawy and Guillemin, 2022). In this study, L-kynurenine and xanthurenic acid in the Kyn pathway were significantly upregulated after chronic heat stress. These findings indicate that the liver of *G. eckloni* can prevent excessive inflammation and induce long-term immune tolerance by activating the Kyn pathway (Sorgdrager et al., 2019). Moreover, the aforementioned metabolites have been shown to act as ROS scavengers and modulate the activity of antioxidant enzymes (Ferrari et al., 2014; Peyrot and Ducrocq, 2008). Trp-2, 3-dioxygenase (TDO) and indoleamine-2,3-dioxygenase (IDO) serve as the initial and rate-limiting enzymes in the Kyn pathway, respectively, and are activated by proinflammatory factors under stress conditions (Yeung et al., 2015). In this study, the decrease observed in the expression of *tdo2* and *ido* in the liver of *G. eckloni* may be attributed to a feedback effect resulting from the accumulation of downstream catabolic metabolites (Lanz et al., 2017). Consistently, studies have demonstrated that inhibiting TDO and the subsequent accumulation of kynurenine exerts a protective effect on the body (Breda et al., 2016;

Maddison and Giorgini, 2015). The tryptophan metabolic pathway serves as the de novo synthesis pathway for NAD, thereby affecting the production of NAD<sup>+</sup> and acetyl-CoA (Bender, 1983). In this study, *acmsd* expression and acetyl-CoA levels were found to be downregulated in the liver of *G. eckloni*. This downregulation may help maintain NAD homeostasis, contributing to the improvement of liver function and alleviation of inflammation (Katsyuba et al., 2018). Indole and its derivatives can regulate the expression of pro-inflammatory and anti-inflammatory cytokines, and their upregulation has been associated with a reduction in the severity of liver injury (Guo et al., 2021; Wang et al., 2022). In this study, the levels of indole-3-ylacetonitrile and indole-3-acetamide were significantly increased, suggesting a decrease in inflammation after heat stress. These findings indicate that tryptophan metabolism plays a crucial role in the adaptation of *G. eckloni* to chronic heat stress. However, further investigation is warranted to understand the mechanisms through which tryptophan metabolism enhances the heat tolerance of *G. eckloni* during aquaculture.

## 5. Conclusion

In this study, we comprehensively assessed the impact of different heat stress conditions on the liver of *G. eckloni* through histopathological examination, morphological analysis, apoptosis assay, assessment of biochemical indices, and transcriptomic and metabolomic analyses. The results showed that heat stress caused liver tissue damage and apoptosis in *G. eckloni*, with the effects of AH being more severe. The antioxidant enzyme CAT was activated to counteract oxidative stress and meet increased energy demands following heat stress. Upregulation of genes associated with protein degradation, such as *hsp40*, *hsp70*, *hsp90*, *ero11*, and *pdi4*, and activation of UPR contributed to the inhibition or elimination of misfolded proteins, which enhanced stress resistance. The differential expression of most metabolites suggested alterations in amino acid metabolism and lipid metabolism in response to heat stress. Notably, integrated transcriptomic and metabolomic analysis revealed that tryptophan metabolism plays an important role in the adaptation of *G. eckloni* to chronic heat stress. Altogether, these findings provide valuable insights into the mechanisms through which cold-water fish such as *G. eckloni* adapt to heat stress and introduce avenues for improving fish cultivation strategies under high-temperature conditions.

## Funding information

This research was supported by the National Natural Science Foundation of China (32160864); the Natural Science Foundation of Chongqing Province of China (CSTB2022NSCQ-MSX0566); the “Special Fund for Youth team of the Southwest University” (SWU-XJPY202302); and the “National Talent Research Grant for 2023” (5330500953). National Natural Science Foundation of China (NSFC) Joint Fund Priority Support Program(U23A20249) .

## CRedit authorship contribution statement

**Suxing Fu:** Investigation, Formal analysis. **Shuhao Bai:** Formal analysis. **Yutong Zhuang:** Formal analysis. **Jian Shen:** Investigation. **Rongzhu Zhou:** Supervision, Conceptualization. **Chaowei Zhou:** Writing – original draft. **Luo Lei:** Supervision, Methodology, Conceptualization. **Yuting Duan:** Visualization, Conceptualization. **Haiping Liu:** Supervision, Methodology. **Junting Li:** Writing – review & editing. **Shidong Liu:** Validation. **Hejiao Li:** Resources. **Yinhua Zhou:** Resources. **Qiming Wang:** Investigation.

## Declaration of Competing Interest

The authors declare that they have no known competing financial interests or personal relationships that could have appeared to influence the work reported in this paper.

## Data Availability

Data will be made available on request.

## Appendix A. Supporting information

Supplementary data associated with this article can be found in the online version at doi:10.1016/j.aqrep.2024.102392.

## References

- Alfonso, S., Gesto, M., Sadoul, B., 2021. Temperature increase and its effects on fish stress physiology in the context of global warming. *J. Fish. Biol.* 98, 1496–1508. <https://doi.org/10.1111/jfb.14599>.
- Badawy, A.A.-B., Guillemin, G.J., 2022. Species Differences in Tryptophan Metabolism and Disposition. *Int J. Tryptophan Res* 15, 11786469221122511. <https://doi.org/10.1177/11786469221122511>.
- Bao, C., Li, Z., Guanque, D., Li, C., Yin, G., He, C., Jin, W., Zhou, Y., Chen, Y., 2023. Comparison and phylogenetic analysis of mitochondrial genomes between *Gymnocypris przewalskii* and *Gymnocypris eckloni*. *Acta Agric. Boreal. -Sin.* 38, 213–226. <https://doi.org/10.7668/hbxb.20193633>.
- Bao, J., Qiang, J., Tao, Y., Li, H., He, J., Xu, P., Chen, D., 2018. Responses of blood biochemistry, fatty acid composition and expression of microRNAs to heat stress in genetically improved farmed tilapia (*Oreochromis niloticus*). *J. Therm. Biol.* 73, 91–97. <https://doi.org/10.1016/j.jtherbio.2018.02.007>.
- Bender, D.A., 1983. Biochemistry of tryptophan in health and disease. *Mol. Asp. Med.* 6, 101–197. [https://doi.org/10.1016/0098-2997\(83\)90005-5](https://doi.org/10.1016/0098-2997(83)90005-5).
- Braakman, I., Hebert, D.N., 2013. Protein Folding in the Endoplasmic Reticulum. *Cold Spring Harb. Perspect. Biol.* 5, a013201. <https://doi.org/10.1101/cshperspect.a013201>.
- Breda, C., Sathyaikumar, K.V., Sograte Idrissi, S., Notarangelo, F.M., Estranero, J.G., Moore, G.G.L., Green, E.W., Kyriacou, C.P., Schwarcz, R., Giorgini, F., 2016. Tryptophan-2,3-dioxygenase (TDO) inhibition ameliorates neurodegeneration by modulation of kynurenine pathway metabolites. *Proc. Natl. Acad. Sci.* 113, 5435–5440. <https://doi.org/10.1073/pnas.1604453113>.
- Cai, L., Wang, L., Song, K., Lu, K., Zhang, C., Rahimnejad, S., 2020. Evaluation of protein requirement of spotted seabass (*Lateolabrax maculatus*) under two temperatures, and the liver transcriptome response to thermal stress. *Aquaculture* 516, 734615. <https://doi.org/10.1016/j.aquaculture.2019.734615>.
- Chen, Y., Liu, Y., Bai, Y., Xu, S., Yang, X., Cheng, B., 2022. Intestinal metabolomics of juvenile lenok (*Brachymystax lenok*) in response to heat stress. *Fish. Physiol. Biochem* 48, 1389–1400. <https://doi.org/10.1007/s10695-022-01128-7>.
- Chen, Y., Wu, X., Li, P., Liu, Y., Song, M., Li, F., Ou, J., Lai, J., 2023b. Integrated metabolomic and transcriptomic responses to heat stress in a high-altitude fish, *Triplophysa siluroides*. *Fish. Shellfish Immunol.* 142, 109118. <https://doi.org/10.1016/j.fsi.2023.109118>.
- Chen, Y., Wu, X., Lai, J., Liu, Y., Song, M., Li, F., Gong, Q., 2023a. Integrated biochemical, transcriptomic and metabolomic analyses provide insight into heat stress response in Yangtze sturgeon (*Acipenser dabryanus*). *Ecotoxicol. Environ. Saf.* 249, 114366. <https://doi.org/10.1016/j.ecoenv.2022.114366>.
- Cheng, T., Chen, J., Dong, X., Yang, Q., Liu, H., Zhang, S., Xie, S., Zhang, W., Deng, J., Tan, B., Chi, S., 2023. Protective effect of steroidal saponins on heat stress in the liver of largemouth bass (*Micropterus salmoides*) revealed by metabolomic analysis. *Aquac. Rep.* 33, 101875. <https://doi.org/10.1016/j.aqrep.2023.101875>.
- Choi, H., Shin, D., Kang, G., Kim, K., Park, J., Hur, G.M., Lee, H.-M., Lim, Y.-J., Park, J.-K., Jo, E.-K., Song, C.-H., 2010. Endoplasmic reticulum stress response is involved in *Mycobacterium tuberculosis* protein ESAT-6-mediated apoptosis. *FEBS Lett.* 584, 2445–2454. <https://doi.org/10.1016/j.febslet.2010.04.050>.
- Costabile, A., Castellano, M., Aversa-Marnai, M., Quartiani, I., Conijeski, D., Perretta, A., Villarino, A., Silva-Álvarez, V., Ferreira, A.M., 2022. A different transcriptional landscape sheds light on Russian sturgeon (*Acipenser gueldenstaedtii*) mechanisms to cope with bacterial infection and chronic heat stress. *Fish. Shellfish Immunol.* 128, 505–522. <https://doi.org/10.1016/j.fsi.2022.08.022>.
- Dagoudo, M., Mutebi, E.T., Qiang, J., Tao, Y.-F., Zhu, H.-J., Ngoepe, T.K., Xu, P., 2023. Effects of acute heat stress on haemato-biochemical parameters, oxidative resistance ability, and immune responses of hybrid yellow catfish (*Pelteobagrus fulvidraco* × *P. vachelli*) juveniles. *Vet. Res Commun.* 47, 1217–1229. <https://doi.org/10.1007/s11259-022-10062-1>.
- Duan, P., Tian, Y., Li, Z., Chen, S., Li, L., Wang, X., Wang, L., Liu, Y., Zhai, J., Li, W., Wang, Q., Ma, W., Pang, Z., 2024. Comparative transcriptome analysis of hybrid Jinhui grouper (*Epinephelus fuscoguttatus* ♀ × *Epinephelus tukula* ♂) and *Epinephelus fuscoguttatus* under temperature stress. *Aquaculture* 578, 740037. <https://doi.org/10.1016/j.aquaculture.2023.740037>.
- Ferrari, R., Pugini, S.M.P., Arce, A.I.C., Costa, E.J.X., de Melo, M.P., 2014. Metabolite of tryptophan promoting changes in EEG signal and the oxidative status of the brain. *Cell Biochem Funct.* 32, 496–501. <https://doi.org/10.1002/cbf.3043>.
- Giroux, M., Gan, J., Schlenk, D., 2019. The effects of bifenthrin and temperature on the endocrinology of juvenile Chinook salmon. *Environ. Toxicol. Chem.* 38, 852–861. <https://doi.org/10.1002/etc.4372>.
- Guo, K., Ruan, G., Fan, W., Wang, Q., Fang, L., Luo, J., Liu, Y., 2020. Immune response to acute heat stress in the intestine of the red swamp crayfish, *Procambarus clarkii*. *Fish. Shellfish Immunol.* 100, 146–151. <https://doi.org/10.1016/j.fsi.2020.03.017>.

- Guo, Y., Liu, Y., Wu, W., Ling, D., Zhang, Q., Zhao, P., Hu, X., 2021. Indoleamine 2,3-dioxygenase (Ido) inhibitors and their nanomedicines for cancer immunotherapy. *Biomaterials* 276, 121018. <https://doi.org/10.1016/j.biomaterials.2021.121018>.
- Gupta, G.S., 2012. Lectins in Quality Control: Calnexin and Calreticulin. In: Gupta, G.S. (Ed.), *Animal Lectins: Form, Function and Clinical Applications*. Springer, Vienna, pp. 29–56. [https://doi.org/10.1007/978-3-7091-1065-2\\_2](https://doi.org/10.1007/978-3-7091-1065-2_2).
- Han, P., Qiao, Y., He, J., Wang, X., 2023. Stress responses to warming in Japanese flounder (*Paralichthys olivaceus*) from different environmental scenarios. *Sci. Total Environ.* 897, 165341. <https://doi.org/10.1016/j.scitotenv.2023.165341>.
- Han, X., Jin, S., Shou, C., Han, Z., 2023. Hsp70 Gene Family in *Sebastes marmoratus*: The genome-wide identification and transcriptome analysis under thermal stress. *Genes* 14, 1779. <https://doi.org/10.3390/genes14091779>.
- Hazel, J.R., 1979. Influence of thermal acclimation on membrane lipid composition of rainbow trout liver. *Am. J. Physiol. -Regul., Integr. Comp. Physiol.* 236, R91–R101. <https://doi.org/10.1152/ajpregu.1979.236.1.R91>.
- He, C., Li, C., Bao, C., Wang, L., Yan, Q., Jin, W., Zhao, J., Wang, G., Jian, S., Wang, Z., Chen, Y., 2024. Cloning and expression analysis of MSTN-I gene in *Gymnocypris eckloni*. *Acta Agric. Boreal. -Sin.* 39, 228–238. <https://doi.org/10.1016/j.aqrep.2023.101538>.
- He, H., Zhang, B., Sun, S., Liu, H., Wang, W., Zhou, J., 2023. Liver transcriptome analysis revealing response to high-temperature stress in *Glyptosternum maculatum* (Sisoridae: Siluriformes). *Aquac. Rep.* 29, 101538. <https://doi.org/10.1016/j.aqrep.2023.101538>.
- Herrera, M., Hervas, M.A., Giráldez, I., Skar, K., Mogren, H., Mortensen, A., Puvanendran, V., 2017. Effects of amino acid supplementations on metabolic and physiological parameters in Atlantic cod (*Gadus morhua*) under stress. *Fish. Physiol. Biochem.* 43, 591–602. <https://doi.org/10.1007/s10695-016-0314-3>.
- Hetz, C., Zhang, K., Kaufman, R.J., 2020. Mechanisms, regulation and functions of the unfolded protein response. *Nat. Rev. Mol. Cell Biol.* 21, 421–438. <https://doi.org/10.1038/s41580-020-0250-z>.
- Holmsen, H., Hindenes, J.O., Fukami, M., 1992. Glycerophospholipid metabolism: back to the future. *Thromb. Res.* 67, 313–323. [https://doi.org/10.1016/0049-3848\(92\)90006-v](https://doi.org/10.1016/0049-3848(92)90006-v).
- Hou, Q., Kwok, L.-Y., Zheng, Y., Wang, L., Guo, Z., Zhang, J., Huang, W., Wang, Y., Leng, L., Li, H., Zhang, H., 2016. Differential fecal microbiota are retained in broiler chicken lines divergently selected for fatness traits. *Sci. Rep.* 6, 37376. <https://doi.org/10.1038/srep37376>.
- Huang, J., Li, Y., Liu, Z., Kang, Y., Wang, J., 2018. Transcriptomic responses to heat stress in rainbow trout *Oncorhynchus mykiss* head kidney. *Fish. Shellfish Immunol.* 82, 32–40. <https://doi.org/10.1016/j.fsi.2018.08.002>.
- Jian, S., Yang, B., Zhao, J., Lv, Z., Li, K., Guan, H., Yin, X., 2020. Technique for raising large scale seedling of *Gymnocypris eckloni* in Qinghai, 24-26+49 Hebei Fish. <https://doi.org/10.3969/j.issn.1004-6755.2020.03.007>.
- Jing, H., Zhou, L., Gao, Y., Liu, Z., Wu, B., Sun, X., Tu, K., 2023. Transcriptomics and metabolomics reveal the molecular and metabolic adaptation to heat stress in Manila clam *Ruditapes philippinarum*. *Front. Mar. Sci.* 10, 1204598. <https://doi.org/10.3389/fmars.2023.1204598>.
- Katsyuba, E., Mottis, A., Zietak, M., De Franco, F., van der Velpen, V., Gariani, K., Ryu, D., Cialabrin, L., Mattilainen, O., Liscio, P., Giacchè, N., Stokar-Regenscheit, N., Legouis, D., de Seigneux, S., Ivanisevic, J., Raffaelli, N., Schoonjans, K., Pellicciari, R., Auwerx, J., 2018. De novo NAD+ synthesis enhances mitochondrial function and improves health. *Nature* 563, 354–359. <https://doi.org/10.1038/s41586-018-0645-6>.
- Kaur, M., Atif, F., Ali, M., Rehman, H., Raisuddin, S., 2005. Heat stress-induced alterations of antioxidants in the freshwater fish *Channa punctata* Bloch. *J. Fish. Biol.* 67, 1653–1665. <https://doi.org/10.1111/j.1095-8649.2005.00872.x>.
- Kim, J.-H., Kim, S.K., Hur, Y.B., 2019. Temperature-mediated changes in stress responses, acetylcholinesterase, and immune responses of juvenile olive flounder *Paralichthys olivaceus* in a bio-floc environment. *Aquaculture* 506, 453–458. <https://doi.org/10.1016/j.aquaculture.2019.03.045>.
- Kühnhold, H., Kamyab, E., Novais, S., Indriana, L., Kunzmann, A., Slater, M., Lemos, M., 2017. Thermal stress effects on energy resource allocation and oxygen consumption rate in the juvenile sea cucumber, *Holothuria scabra* (Jaeger, 1833). *Aquaculture*. *Cut. Edge Sci. Aquac.* 2015 467, 109–117. <https://doi.org/10.1016/j.aquaculture.2016.03.018>.
- Langston, A.L., Hoare, R., Stefansson, M., Fitzgerald, R., Wergeland, H., Mulcahy, M., 2002. The effect of temperature on non-specific defence parameters of three strains of juvenile Atlantic halibut (*Hippoglossus hippoglossus* L.). *Fish. Shellfish Immunol.* 12, 61–76. <https://doi.org/10.1006/fsim.2001.0354>.
- Lanz, T.V., Williams, S.K., Stojic, A., Iwantschew, S., Sonner, J.K., Grabitz, C., Becker, S., Böhrler, L.-I., Mohapatra, S.R., Sahm, F., Küblbeck, G., Nakamura, T., Funakoshi, H., Opitz, C.A., Wick, W., Diem, R., Platten, M., 2017. Tryptophan-2,3-Dioxygenase (TDO) deficiency is associated with subclinical neuroprotection in a mouse model of multiple sclerosis. *Sci. Rep.* 7, 41271. <https://doi.org/10.1038/srep41271>.
- Li, B., Sun, S., Zhu, J., Yanli, S., Wuxiao, Z., Ge, X., 2019. Transcriptome profiling and histology changes in juvenile blunt snout bream (*Megalobrama amblycephala*) liver tissue in response to acute thermal stress. *Genomics* 111, 242–250. <https://doi.org/10.1016/j.ygeno.2018.11.011>.
- Li, C., Wang, Y., Wang, G., Chen, Y., Guo, J., Pan, C., Liu, E., Ling, Q., 2019. Physicochemical changes in liver and Hsc70 expression in pikeperch *Sander lucioperca* under heat stress. *Ecotoxicol. Environ. Saf.* 181, 130–137. <https://doi.org/10.1016/j.ecoenv.2019.05.083>.
- Li, H., Deng, L., 2014. Mineral analysis and nutritional value evaluation of *Gymnocypris eckloni*. *Sichuan J. Zool.* 33, 923–925. <https://doi.org/10.3969/j.issn.1000-7083.2014.06.020>.
- Li, J., Duan, Y., Kong, W., Gao, H., Fu, S., Li, H., Zhou, Y., Liu, H., Yuan, D., Zhou, C., 2024. Heat stress affects swimming performance and induces biochemical, structural, and transcriptional changes in the heart of *Gymnocypris eckloni*. *Aquac. Rep.* 35, 101998. <https://doi.org/10.1016/j.aqrep.2024.101998>.
- Li, L., Liu, Z., Quan, J., Lu, J., Zhao, G., Sun, J., 2022. Dietary nanoselenium supplementation for heat-stressed rainbow trout: effects on organizational structure, lipid changes, and biochemical parameters as well as heat-shock-protein- and selenoprotein-related gene expression. *Fish. Physiol. Biochem.* 48, 707–722. <https://doi.org/10.1007/s10695-022-01084-2>.
- Li, P., Li, Z.-H., Zhong, L., 2019. Triphenyltin exposure alters the antioxidant system, energy metabolism and the expression of genes related to physiological stress in zebrafish (*Danio rerio*). *Comp. Biochem. Physiol. Part C: Toxicol. Pharmacol.* 225, 108581. <https://doi.org/10.1016/j.cbpc.2019.108581>.
- Li, Y., Huang, J., Liu, Z., Zhou, Y., Xia, B., Wang, Y., Kang, Y., Wang, J., 2017. Transcriptome analysis provides insights into hepatic responses to moderate heat stress in the rainbow trout (*Oncorhynchus mykiss*). *Gene* 619, 1–9. <https://doi.org/10.1016/j.gene.2017.03.041>.
- Li, Z., Zhao, Z., Luo, L., Wang, S., Zhang, R., Guo, K., Yang, Y., 2023. Immune and intestinal microbiota responses to heat stress in Chinese mitten crab (*Eriocheir sinensis*). *Aquaculture* 563, 738965. <https://doi.org/10.1016/j.aquaculture.2022.738965>.
- Lin, Y., Miao, L., Pan, W.-J., Huang, X., Deng, J.M., Zhang, W., Ge, X., Liu, B., Ren, M., Zhou, Q., Xie, J., Pan, L., Xi, B., 2018. Effect of nitrite exposure on the antioxidant enzymes and glutathione system in the liver of bighead carp, *Aristichthys nobilis*. *Fish. Shellfish Immunol.* 76, 126–132. <https://doi.org/10.1016/j.fsi.2018.02.015>.
- Liu, A., Pirozzi, I., Codabaccus, B.M., Sammut, J., Booth, M.A., 2021. The interactive effect of dietary choline and water temperature on the liver lipid composition, histology, and plasma biochemistry of juvenile yellowtail kingfish (*Seriola lalandi*). *Aquaculture* 531, 735893. <https://doi.org/10.1016/j.aquaculture.2020.735893>.
- Liu, B., Xu, P., Brown, P.B., Xie, J., Ge, X., Miao, L., Zhou, Q., Ren, M., Pan, L., 2016. The effect of hyperthermia on liver histology, oxidative stress and disease resistance of the Wuchang bream, *Megalobrama amblycephala*. *Fish. Shellfish Immunol.* 52, 317–324. <https://doi.org/10.1016/j.fsi.2016.03.018>.
- Liu, E., Zhao, X., Li, C., Wang, Y., Li, L., Zhu, H., Ling, Q., 2022. Effects of acute heat stress on liver damage, apoptosis and inflammation of pikeperch (*Sander lucioperca*). *J. Therm. Biol.* 106, 103251. <https://doi.org/10.1016/j.jtherbio.2022.103251>.
- Liu, F., Zhang, T., He, Y., Zhan, W., Xie, Q., Lou, B., 2023. Integration of transcriptome and proteome analyses reveals the regulation mechanisms of *Larimichthys polyactis* liver exposed to heat stress. *Fish. Shellfish Immunol.* 135, 108704. <https://doi.org/10.1016/j.fsi.2023.108704>.
- Liu, H., Yang, R., Fu, Z., Yu, G., Li, M., Dai, S., Ma, Z., Zong, H., 2023. Acute thermal stress increased enzyme activity and muscle energy distribution of yellowfin tuna. *PLOS ONE* 18, e0289606. <https://doi.org/10.1371/journal.pone.0289606>.
- Liu, Z., Suo, C., Jiang, Y., Zhao, R., Zhang, T., Jin, L., Chen, X., 2022. Phenome-wide association analysis reveals novel links between genetically determined levels of liver enzymes and disease phenotypes. *Phenomics* 2, 295–311. <https://doi.org/10.1007/s43657-021-00033-y>.
- Livak, K.J., Schmittgen, T.D., 2001. Analysis of relative gene expression data using real-time quantitative PCR and the 2<sup>-ΔΔCT</sup> method. *Methods* 25, 402–408. <https://doi.org/10.1006/meth.2001.1262>.
- Long, Z., Qin, H., Huang, Z., Xu, A., Ye, Y., Li, Z., 2023. Effects of heat stress on physiological parameters, biochemical parameters and expression of heat stress protein gene in *Lateolabrax maculatus*. *J. Therm. Biol.* 115, 103606. <https://doi.org/10.1016/j.jtherbio.2023.103606>.
- Lu, J., Shi, Y., Cai, S., Feng, J., 2017. Metabolic responses of *Haliotis diversicolor* to *Vibrio parahaemolyticus* infection. *Fish. Shellfish Immunol.* 60, 265–274. <https://doi.org/10.1016/j.fsi.2016.11.051>.
- Lu, S., Xian, T., Wang, D., Wang, C., Liu, Y., Liu, H., Han, S., 2022. Effects of traditional Chinese medicines on biochemical parameters, antioxidant capacity and heat shock protein expression in rainbow trout (*Oncorhynchus mykiss*) under heat stress. *Aquac. Res.* 53, 6148–6157. <https://doi.org/10.1111/are.16088>.
- Lu, Y., Wu, Z., Song, Z., Xiao, P., Liu, Y., Zhang, P., You, F., 2016. Insight into the heat resistance of fish via blood: effects of heat stress on metabolism, oxidative stress and antioxidant response of olive flounder *Paralichthys olivaceus* and turbot *Scophthalmus maximus*. *Fish. Shellfish Immunol.* 58, 125–135. <https://doi.org/10.1016/j.fsi.2016.09.008>.
- Ma, D., Fan, J., Zhu, H., Su, H., Jiang, P., Yu, L., Liao, G., Bai, J., 2020. Histologic examination and transcriptome analysis uncovered liver damage in largemouth bass from formulated diets. *Aquaculture* 526, 735329. <https://doi.org/10.1016/j.aquaculture.2020.735329>.
2015. Maddison, D.C., Giorgini, F., 2015. The kynurenine pathway and neurodegenerative disease. *Seminars in Cell & Developmental Biology, Extracellular vesicles: a paradigm shift in how we think about cell-cell communication & Molecular neuroprotection* 40, 134–141. <https://doi.org/10.1016/j.semcdb.2015.03.002>.
- Mahanty, A., Mohanty, S., Mohanty, B.P., 2017. Dietary supplementation of curcumin augments heat stress tolerance through upregulation of nrf-2-mediated antioxidative enzymes and hsp in *Puntius sophore*. *Fish. Physiol. Biochem.* 43, 1131–1141. <https://doi.org/10.1007/s10695-017-0358-z>.
- Mahanty, A., Purohit, G.K., Mohanty, S., Mohanty, B.P., 2019. Heat stress-induced alterations in the expression of genes associated with gonadal integrity of the teleost *Puntius sophore*. *Fish. Physiol. Biochem.* 45, 1409–1417. <https://doi.org/10.1007/s10695-019-00643-4>.
- Mahmoud, M.A., Kassab, M.S., Zaineldin, A.I., Amer, A.A., Gewaily, M.S., Darwish, S., Dawood, M.A.O., 2023. Mitigation of Heat Stress in Striped Catfish (*Pangasianodon hypophthalmus*) by Dietary Alicin: Exploring the Growth Performance, Stress

- Biomarkers, Antioxidative, and Immune Responses. *Aquac. Res.* 2023, e8292007. <https://doi.org/10.1155/2023/8292007>.
- Mahmoud, S., Sabry, A., Abdelaziz, A., Shukry, M., 2020. Deleterious impacts of heat stress on steroidogenesis markers, immunity status and ovarian tissue of Nile tilapia (*Oreochromis niloticus*). *J. Therm. Biol.* 91, 102578. <https://doi.org/10.1016/j.jtherbio.2020.102578>.
- Melvin, S.D., Lancôt, C.M., Doriean, N.J.C., Bennett, W.W., Carroll, A.R., 2019. NMR-based lipidomics of fish from a metal(loids) contaminated wetland show differences consistent with effects on cellular membranes and energy storage. *Sci. Total Environ.* 654, 284–291. <https://doi.org/10.1016/j.scitotenv.2018.11.113>.
- Naz, Saima, Iqbal, S., Khan, R.U., Chatha, A.M.M., Naz, Shabana, 2023. Aquaculture Fish Responses Towards Temperature Stress: A Critical Review. In: Ahmad, Md.I., Mahamood, M., Javed, M., Alhewairini, S.S. (Eds.), *Toxicology and Human Health: Environmental Exposures and Biomarkers*. Springer Nature, Singapore, pp. 83–132. [https://doi.org/10.1007/978-981-99-2193-5\\_5](https://doi.org/10.1007/978-981-99-2193-5_5).
- Peyrot, F., Ducrocq, C., 2008. Potential role of tryptophan derivatives in stress responses characterized by the generation of reactive oxygen and nitrogen species. *J. Pineal Res* 45, 235–246. <https://doi.org/10.1111/j.1600-079X.2008.00580.x>.
- Plempner, R.K., Böhmeler, S., Bordallo, J., Sommer, T., Wolf, D.H., 1997. Mutant analysis links the translocon and BiP to retrograde protein transport for ER degradation. *Nature* 388, 891–895. <https://doi.org/10.1038/42276>.
- Qaid, M.M., Al-Garadi, M.A., 2021. Protein and amino acid metabolism in poultry during and after heat stress: a review. *Animals* 11, 1167. <https://doi.org/10.3390/ani11041167>.
- Qin, H., Long, Z., Huang, Z., Ma, J., Kong, L., Lin, Y., Lin, H., Zhou, S., Li, Z., 2023. A Comparison of the physiological responses to heat stress of two sizes of juvenile spotted seabass (*Lateolabrax maculatus*). *Fishes* 8, 340. <https://doi.org/10.3390/fishes8070340>.
- Ran, F., Jin, W., Duanzhi, Z., Huang, S., Liu, Y., Li, Z., Wang, Z., Wu, M., Jian, S., Wang, G., Li, C., 2021. Effects of Zn<sup>2+</sup> stress on expression of key antioxidant genes and antioxidant enzyme activities in eckloni naked carp *Gymnocypris eckloni*. *J. Dalian Ocean Univ.* 36, 406–413. <https://doi.org/10.16535/j.cnki.dlhyxb.2020-147>.
- Sahu, S., Ngsotter, S., Mog, M., Tesia, S., Sharma, S., Dayakar, B., Waikhom, D., 2020. A review on physiological, behavioral and metabolic role of dietary tryptophan in fish. *Int. J. Chem. Sci.* 8, 2411–2417. <https://doi.org/10.22271/chemi.2020.v8.i3ai.9571>.
- Sissener, N. h, Torstensen, B. e, Owen, M. a g, Liland, N. s, Stubhaug, I., Rosenlund, G., 2017. Temperature modulates liver lipid accumulation in Atlantic salmon (*Salmo salar* L.) fed low dietary levels of long-chain n-3 fatty acids. *Aquac. Nutr.* 23, 865–878. <https://doi.org/10.1111/anu.12453>.
- Sokolova, I.M., Frederich, M., Bagwe, R., Lannig, G., Sukhotin, A.A., 2012. Energy homeostasis as an integrative tool for assessing limits of environmental stress tolerance in aquatic invertebrates. *Mar. Environ. Res.* 79, 1–15. <https://doi.org/10.1016/j.marenvres.2012.04.003>.
- Sorgdrager, F.J.H., Naudé, P.J.W., Kema, I.P., Nollen, E.A., Deyn, P.P.D., 2019. Tryptophan Metabolism in Inflammaging: From Biomarker to Therapeutic Target. *Front. Immunol.* 10. <https://doi.org/10.3389/fimmu.2019.02565>.
- Su, R., Fang, J., Wang, H., Liu, B., 2021. Lipid metabolism changes in clam *Meretrix petechialis* in response to *Vibrio* infection and the identification of *Vibrio*-resistance markers. *Aquaculture* 539, 736611. <https://doi.org/10.1016/j.aquaculture.2021.736611>.
- Tang, Y., Peng, X., Fang, J., Cui, H.-M., Zuo, Z.-C., Deng, J.-L., 2015. Characterization of hematological parameters and blood cells of cultured *Gymnocypris eckloni* Herzenstein, 1891. *J. Appl. Ichthyol.* 31, 931–936. <https://doi.org/10.1111/jai.12798>.
- Wang, F., Wang, L., Liu, D., Gao, Q., Nie, M., Zhu, S., Chao, Y., Yang, C., Zhang, C., Yi, R., Ni, W., Tian, F., Zhao, K., Qi, D., 2022. Chromosome-level assembly of *Gymnocypris eckloni* genome. *Sci. Data* 9, 1–8. <https://doi.org/10.1038/s41597-022-01595-w>.
- Wang, J., Jiang, X., Sun, Z., 2022. Length weight relationships of commercial fishes from the mainstream of Yellow River, China. *Pak. J. Zool.* 54, 2985–2987. <https://doi.org/10.17582/journal.pjz/20210924030907>.
- Wang, M., Zhao, S., Wang, J., Nie, L., Li, L., Zhu, X., Zhang, L., 2024. Multi-omics analysis provides insight into liver metabolism in yellow catfish (*Pelteobagrus fulvidraco*) under hypoxic stress. *Aquaculture* 583, 740531. <https://doi.org/10.1016/j.aquaculture.2023.740531>.
- Wang, S., Zheng, Y., Chen, M., Storey, K.B., 2021. Ultrastructural variation and key ER chaperones response induced by heat stress in intestinal cells of sea cucumber *Apostichopus japonicus*. *J. Ocean. Limnol.* 39, 317–328. <https://doi.org/10.1007/s00343-020-9265-8>.
- Wang, W., Gao, L., Liu, W., Tian, Z., Wang, X., Hu, H., 2023. Regulation of antioxidant defense in response to heat stress in Siberian sturgeon (*Acipenser baerii*). *Aquaculture* 572, 739551. <https://doi.org/10.1016/j.aquaculture.2023.739551>.
- Wang, X., Wang, Xiaodong, Peng, C., Shi, H., Yang, J., He, M., Zhang, M., Zhou, Y., Duan, L., 2022. Exogenous gamma-aminobutyric acid coordinates active oxygen and amino acid homeostasis to enhance heat tolerance in wheat seedlings. *J. Plant Growth Regul.* 41, 2787–2797. <https://doi.org/10.1007/s00344-021-10474-4>.
- Wang, X.-N., Xia, W.-R., Liu, J.-Q., Sun, F.-Y., Zhong, Z.-J., Liu, L.-F., Xin, G.-Z., 2022. Targeting tryptophan metabolism reveals Clematichinenoside AR alleviates triptolide-induced hepatotoxicity. *J. Pharm. Biomed. Anal.* 208, 114461. <https://doi.org/10.1016/j.jpba.2021.114461>.
- Wang, Y., Li, C., Pan, C., Liu, E., Zhao, X., Ling, Q., 2019. Alterations to transcriptomic profile, histopathology, and oxidative stress in liver of pikeperch (*Sander lucioperca*) under heat stress. *Fish. Shellfish Immunol.* 95, 659–669. <https://doi.org/10.1016/j.fsi.2019.11.014>.
- Wolf, J.C., Baumgartner, W.A., Blazer, V.S., Camus, A.C., Engelhardt, J.A., Fournie, J.W., Frasca, S., Groman, D.B., Kent, M.L., Khoo, L.H., Law, J.M., Lombardini, E.D., Ruehl-Fehlert, C., Segner, H.E., Smith, S.A., Spitsbergen, J.M., Weber, K., Wolfe, M.J., 2015. Nonlesions, misdiagnoses, missed diagnoses, and other interpretive challenges in fish histopathology studies: a guide for investigators, authors, reviewers, and readers. *Toxicol. Pathol.* 43, 297–325. <https://doi.org/10.1177/0192623314540229>.
- Wu, Z., Yang, Y., Zhou, L., Chi, C., Sun, X., Wu, B., Liu, Z., Wang, Y., 2023. Transcriptome sequencing reveals the response to acute thermal stress in the pacific abalone, *Haliotis discus hannai*. *Aquac. Res.* 2023, e7621215. <https://doi.org/10.1155/2023/7621215>.
- Xue, C., Li, G., Zheng, Q., Gu, X., Shi, Q., Su, Y., Chu, Q., Yuan, X., Bao, Z., Lu, J., Li, L., 2023. Tryptophan metabolism in health and disease. *Cell Metab.* 35, 1304–1326. <https://doi.org/10.1016/j.cmet.2023.06.004>.
- Yang, L., Fang, J., Peng, X., Cui, H., He, M., Zuo, Z., Zhou, Y., Yang, Z., 2017. Study on the morphology, histology and enzymatic activity of the digestive tract of *Gymnocypris eckloni* Herzenstein. *Fish. Physiol. Biochem.* 43, 1175–1185. <https://doi.org/10.1007/s10695-017-0363-2>.
- Yang, S., Zhao, T., Ma, A., Huang, Z., Liu, Z., Cui, W., Zhang, J., Zhu, C., Guo, X., Yuan, C., 2020. Metabolic responses in *Scophthalmus maximus* kidney subjected to thermal stress. *Fish. Shellfish Immunol.* 103, 37–46. <https://doi.org/10.1016/j.fsi.2020.04.003>.
- Yeung, A.W.S., Terentis, A.C., King, N.J.C., Thomas, S.R., 2015. Role of indoleamine 2,3-dioxygenase in health and disease. *Clin. Sci. (Lond.)* 129, 601–672. <https://doi.org/10.1042/CS20140392>.
- Zhang, H., Xu, B., A. L., Ma, Q., Gao, Q., Tian, W., Yu, L., Liang, J., n.d. Cloning, tissue expression and polymorphism of MHCII gene of *Gymnocypris przewalskii* and *Gymnocypris eckloni*. *Journal of Fisheries of China* 1–17.
- Zhang, L., Wang, Y., Jia, H., Liu, X., Zhang, R., Guan, J., 2023. Transcriptome and metabolome analyses reveal the regulatory effects of compound probiotics on cecal metabolism in heat-stressed broilers. *Poult. Sci.* 102, 102323. <https://doi.org/10.1016/j.psj.2022.102323>.
- Zhang, W., Pang, A., Tan, B., Xin, Y., Liu, Y., Xie, R., Zhang, H., Yang, Q., Deng, J., Chi, S., 2022. Tryptophan metabolism and gut flora profile in different soybean protein induced enteritis of pearl gentian groupers. *Front. Nutr.* 9. <https://doi.org/10.3389/fnut.2022.1014502>.
- Zhang, X., Yu, H., Yan, X., Li, P., Wang, C., Zhang, C., Ji, H., Gao, Q., Dong, S., 2022. Selenium improved mitochondrial quality and energy supply in the liver of high-fat diet-fed grass carp (*Ctenopharyngodon idella*) after heat stress. *Fish. Physiol. Biochem* 48, 1701–1716. <https://doi.org/10.1007/s10695-022-01140-x>.
- Zhao, T., Ma, A., Huang, Z., Liu, Z., Sun, Z., Zhu, L., Chang, H., 2024. ppar $\beta$  regulates lipid catabolism by mediating acox and cpt-1 genes in *Scophthalmus maximus* under heat stress. *Fish. Physiol. Biochem* 50, 295–305. <https://doi.org/10.1007/s10695-024-01313-w>.
- Zhao, X., Li, L., Li, C., Liu, E., Zhu, H., Ling, Q., 2022. Heat stress-induced endoplasmic reticulum stress promotes liver apoptosis in largemouth bass (*Micropterus salmoides*). *Aquaculture* 546, 737401. <https://doi.org/10.1016/j.aquaculture.2021.737401>.
- Zhao, Y., Wu, R., Yao, Y., Chen, Q., Xia, M., Qi, D., 2018. cDNA cloning and hypoxia-induced mRNA expression of Epo and Epor genes in *Gymnocypris eckloni*. *Chin. J. Zool.* 53, 220–233. <https://doi.org/10.13859/j.cjz.201802007>.
- Zhou, C., Gao, P., Wang, J., 2023. Comprehensive analysis of microbiome, metabolome, and transcriptome revealed the mechanisms of intestinal injury in rainbow trout under heat stress. *Int. J. Mol. Sci.* 24, 8569. <https://doi.org/10.3390/ijms24108569>.